



Design, synthesis and anticancer/antiestrogenic activities of novel indole-benzimidazoles

Fikriye Zengin Karadayi^{a,1}, Murat Yaman^{c,1}, Mehmet Murat Kisla^{a,2}, Ayse G. Keskus^{c,2}, Ozlen Konu^{b,c,d,*}, Zeynep Ates-Alagoz^{a,*}

^a Department of Pharmaceutical Chemistry, Faculty of Pharmacy, Ankara University, 06100 Ankara, Turkey

^b Department of Molecular Biology and Genetics, Bilkent University, 06800 Ankara, Turkey

^c Interdisciplinary Program in Neuroscience, Bilkent University, 06800 Ankara, Turkey

^d UNAM-Institute of Materials Science and Nanotechnology, Bilkent University, 06800 Ankara, Turkey

ARTICLE INFO

InChIKeys:

NKANXQFJJICGDU-QPLCGJKRSA-N

GZUITABIAMVPG-UHFFFAOYSA-N

UCJGJABZCDBEDK-UHFFFAOYSA-N

Indole-benzimidazole

Molecular docking

Comparative transcriptomics

Estrogen signaling

ABSTRACT

Indole-benzimidazoles have recently gained attention due to their antiproliferative and antiestrogenic effects. However, their structural similarities and molecular mechanisms shared with selective estrogen receptor modulators (SERMs) have not yet been investigated. In this study, we synthesized novel ethylsulfonyl indole-benzimidazole derivatives by substituting the first (R₁) and fifth (R₂) positions of benzimidazole and indole groups, respectively. Subsequently, we performed ¹H NMR, ¹³C NMR, and Mass spectral and *in silico* docking analyses, and anticancer activity screening studies of these novel indole-benzimidazoles. The antiproliferative effects of indole-benzimidazoles were found to be more similar between the estrogen (E2) responsive cell lines MCF-7 and HEPG2 in comparison to the Estrogen Receptor negative (ER-) cell line MDA-MB-231. R₁:p-fluorobenzyl group members were selected as lead compounds for their potent anticancer effects and moderate structural affinity to ER. Microarray expression profiling and gene enrichment analyses (GSEA) of the selected compounds (R₁:p-fluorobenzyl: **48**, **49**, **50**, **51**; R₁:3,4-difluorobenzyl: **53**) helped determine the similarly modulated cellular signaling pathways among derivatives. Moreover, we identified known compounds that have significantly similar gene signatures to that of **51** via queries performed in LINCS database; and further transcriptomics comparisons were made using public GEO datasets (GSE35428, GSE7765, GSE62673). Our results strongly demonstrate that these novel indole-benzimidazoles can modulate ER target gene expression as well as dioxin-mediated aryl hydrocarbon receptor and amino acid deprivation-mediated integrated stress response signaling in a dose-dependent manner.

1. Introduction

Breast cancer, which is among the most prevalent cancer types affecting women all over the world, can be conventionally subtyped according to the presence of estrogen receptor (ER), progesterone receptor (PR), and/or human epidermal growth factor receptor 2 (HER2/ERBB2) activity. These subtypes possess differential characteristics regarding prognosis, incidence, therapeutic response and tumor aggressiveness. The heterogeneous nature and adverse effects associated with therapeutic targeting of such diverse and crucial pathways bring challenges into the therapy and hence makes the discovery of novel, more effective, and subtype specific anticancer molecules invaluable [1].

Estrogens (E2) play crucial roles in breast cancer development, consequently a considerable amount of research has been done either to block their synthesis or to modulate their activity [2]. Therefore, drugs that function as antiestrogens in mammary tissue have been frequently used for the treatment of hormone-dependent breast cancers. Nuclear receptors ER α and ER β , through E2 binding, take part in multiple cellular activities such as proliferation and differentiation. In addition, they can be found at an equilibrium [2–4] and differentially regulate their downstream elements upon exposure to selective estrogen receptor modulators (SERMs) [5]. Moreover, their expression levels differ among various tissues while the expression of ER α is tightly associated with breast cancer physiology [6] as well as prognosis of breast tumors

* Corresponding authors at: Department of Pharmaceutical Chemistry, Faculty of Pharmacy, Ankara University, 06100 Ankara, Turkey (Z. Ates-Alagoz), Department of Molecular Biology and Genetics, Bilkent University, 06800 Ankara, Turkey (O. Konu).

E-mail addresses: konu@fen.bilkent.edu.tr (O. Konu), zeynep.ates@pharmacy.ankara.edu.tr (Z. Ates-Alagoz).

¹ Equal contributors.

² Equal contributors.

<https://doi.org/10.1016/j.bioorg.2020.103929>

Received 27 March 2020; Received in revised form 6 May 2020; Accepted 8 May 2020

Available online 17 May 2020

0045-2068/ © 2020 Elsevier Inc. All rights reserved.

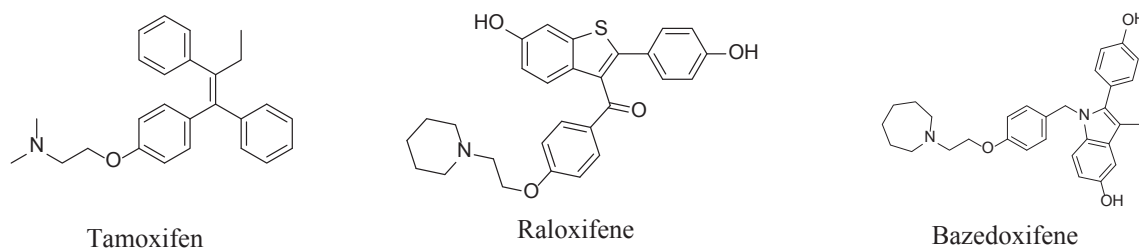
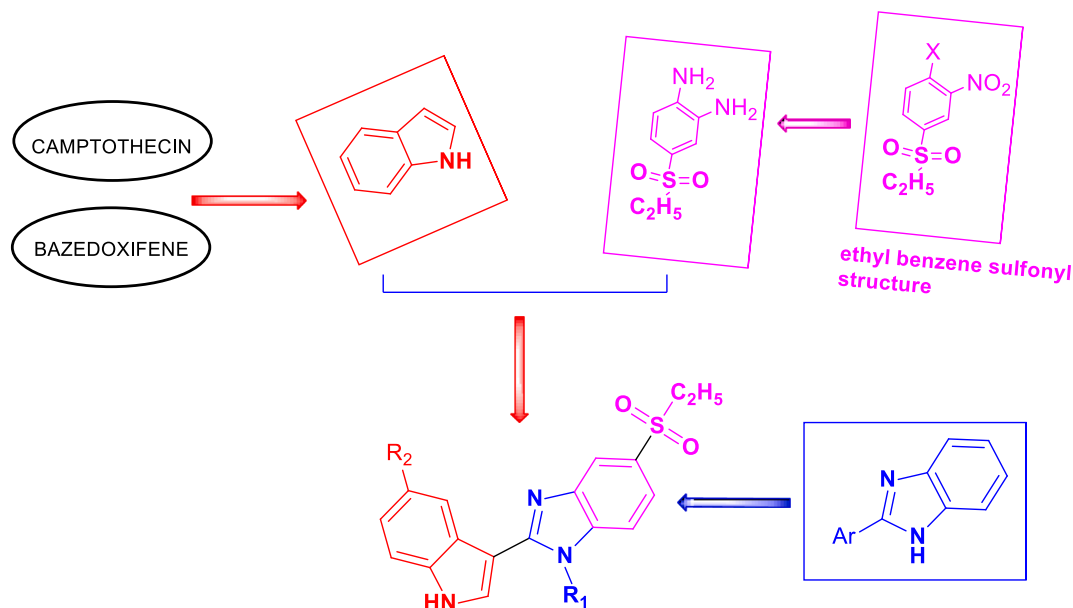


Fig. 1. Chemical structure of tamoxifen, raloxifene and bazedoxifene.



Scheme 1. Scheme showing previous studies and starting point of the new syntheses.

[7]. ER β on the other hand has been implicated in tumor suppression and breast carcinogenesis [8].

Multiple SERMs have been designed and assessed over the years for breast cancer treatment [9]. Moreover, ER α and ER β binding affinities and downstream effects of these SERMs might differ leading to variable outcomes [5,10,11]. Accordingly, tamoxifen (Fig. 1) belonging to the first generation of SERMs has been shown to significantly reduce the incidence of breast cancer. Raloxifene (Fig. 1) is a second-generation SERM exhibiting a role similar to tamoxifen yet it functions as a pure antagonist in the uterus and a partial agonist against tamoxifen-resistant breast cancers [12]. ICI 182780 acts antagonistically in ER positive (ER+) MCF-7 cells and can outperform raloxifene [13]. A third-generation SERM called bazedoxifene (Fig. 1) that has been introduced for the treatment of breast cancer and osteoporosis [14] is based on the pharmacophore of raloxifene. Indole based derivatives (bazedoxifene, melatonin and KB9520), as well as methyl and naphthyl-substituted benzimidazole derivatives also exhibit different modes of actions on breast cancer cell lines some of which could be through actions similar to SERMs [2,15–17]. Accordingly, a combination of affinity studies with toxicological approaches as well as molecular profiling could be highly beneficial to help identify more selective/effective breast cancer therapeutic agents [18–21].

Indole and benzimidazole rings, which are bioavailable molecules, constitute structures found in current drugs. These two ring structures are also isosteres of DNA bases that carry purine and pyrimidine cores, and they can as well be purine antimetabolites. For this reason, indole and benzimidazole rings are thought to interact easily with biopolymers in biosystems [22]. Benzimidazole and its derivatives are effective agents against cancer [23,24], inflammation [25] and oxidative stress [26,27] while also having antiviral [28] and antibacterial [28–30] effects. Indole core has already been used to obtain novel derivatives with

antiproliferative activity [31,32]. Aside from several crucial bioactive compounds (tryptophan, serotonin and melatonin), some of the anti-neoplastic compounds, such as vinblastine sulfate, vincristine sulfate, vinorelbine ditartrate and lanreotide carry indole ring systems [33]. In addition, phenyl-indole derivatives have been shown to inhibit breast cancer development through different mechanisms [34–36]. Similarly, recent studies on benzimidazoles reveal that different heterocycles at 2-position yield to potent anticancer agents for various carcinoma cell lines [37,38]. Furthermore, indole-benzimidazole hybrids have been designed and synthesized by fusing the indole nucleus with benzimidazole to develop novel selective ER modulators. These indole-benzimidazoles can represent novel potent ER α antagonist properties and provide promising insight into the discovery of novel SERMs for the management of breast cancer [39]. For instance, in our previous studies, we have discovered a small molecule with benzene sulfonyl structure exhibiting selectivity toward breast cancer cells while sparing normal surrounding cells [40]. Also, benzene sulfonyl structures have been shown to exhibit higher anticancer activity than doxorubicin in breast and prostate cancers [41,42]. However, the molecular mechanism of action of novel indole-benzimidazoles carrying benzene sulfonyl structures has not yet been assessed. Because of the above and the need for new compounds with better anticancer and anti-estrogenic properties, we designed, synthesized and tested a series of indole-benzimidazoles possessing ethylsulfonyl moiety (Scheme 1).

2. Material and methods

2.1. Chemistry

Melting points were determined with Buchi SMP-20 (BuchiLabortechnik, Flawil, Switzerland) and Electrotermal 9100

capillary melting point apparatus (Electrothermal, Essex, U.K.) and are uncorrected. The ^1H NMR spectra in $\text{DMSO}-d_6$ using Varian Mercury-400 FT-NMR spectrometer (Varian Inc., Palo Alto, CA, USA), and the Mass spectra based on ESI(+) method using Waters ZQ micromass LC-MS spectrometer (Waters Corporation, Milford, MA, USA) were recorded. For elemental analysis we used LECO 932 CHNS (Leco-932, St. Joseph, MI, USA) instrument. Silica gel 60 (40–63 mm particle size) was used for column chromatography.

2.1.1. General procedure for synthesis of 3–12

To a solution of 4-(ethylsulfonyl)-1-chloro-2-nitrobenzene (**2**) (5 mmol) in ethanol (5 mL), amine derivative (15 mmol) was added and heated under reflux, until the starting material was consumed (determined by TLC, 8–48 h). Upon cooling the mixture, water was added. The resultant yellow residue was crystallized from ethanol or purified by column chromatography (cc) by using a mixture of hexane and ethyl acetate in varying concentrations as eluent (Table 1) [43].

2.1.2. General procedure for synthesis of 13–22

Compounds **3–12** (3.5 mmol) in EtOH (75 mL) reduced by hydrogenation using 40 psi of H_2 and 10% Pd/C (40 mg) until cessation of H_2 uptake to obtain the catalyst before filtering off on a bed of celite and washing with EtOH; and concentrating the filtrate in vacuo [44]. The crude amine was used without purification (Table 1).

2.1.3. General procedure for synthesis of 23–59

A mixture of the appropriate o-phenylenediamine (1 mmol), related indole derivative (1 mmol) and $\text{Na}_2\text{S}_2\text{O}_5$ (40%) (2 mL) in EtOH (4 mL), was refluxed until starting materials were consumed (determined by TLC, 4–12 h). The precipitate was obtained upon pouring the reaction mixture and then filtering and washing. The residue was purified by column chromatography to give final product [45].

2.1.3.1. 5-(ethylsulfonyl)-2-(1H-indole-3-yl)-1H-benzo[d]imidazole (23). Compound **23** was prepared according to general methods starting from 4-ethylsulfonyl-benzene-1,2-diamine (1.35 mmol, 0.27 g) and indole-3-carboxaldehyde (1.35 mmol, 0.195 g). The residue was purified by cc using the mixture of ethyl acetate-hexane (1:1) as eluent to give a light yellow solid, m.p. 157 °C (0.058 g, 13% yield). ^1H NMR (400 MHz, $\text{DMSO}-d_6$): δ ppm 1.10 (t, 3H), 3.27 (q, 2H), 7.23 (dd, $J = 8.8$ Hz, $J = 2$ Hz, 1H), 7.53 (d, $J = 8.8$ Hz, 1H), 7.64 (m, 2H), 7.83–8.26 (m, 3H), 8.51 (d, $J = 1.6$ Hz, 1H), 11.91 (brd s, 1H, NH), 12.99 (brd d, 1H, NH). ^{13}C NMR (CD_3OD): 8.02, 52.02, 106.93, 113.20, 114.42, 121.25, 123.03, 124.36, 125.67, 127.47, 128.20, 129.74, 132.78, 132.90, 136.59, 136.96, 154.36. MS (ESI+) m/z : 326. $\text{C}_{17}\text{H}_{15}\text{N}_3\text{O}_2\text{S}\cdot 0.9\text{H}_2\text{O}$: C, 59.77; H, 4.95; N, 12.30; S, 9.38 and found C, 59.42; H, 5.23; N, 11.91; S, 9.10.

2.1.3.2. 2-(5-bromo-1H-indol-3-yl)-5-(ethylsulfonyl)-1H-benzo[d]imidazole (24). Compound **24** was prepared according to general methods starting from 4-ethylsulfonyl-benzene-1,2-diamine (0.87 mmol, 0.175 g) and 5-bromo-indole-3-carboxaldehyde (0.87 mmol, 0.195 g). The residue was purified by cc using the chloroform/ethyl acetate (1:1) as eluent to give a white solid, m.p. 192 °C (0.128 g, 36% yield). ^1H NMR (400 MHz, $\text{DMSO}-d_6$): δ ppm 1.11 (t, 3H), 3.29 (q, 2H), 7.37 (d, $J = 8.4$ Hz, 1H), 7.51 (d, $J = 8.8$ Hz, 1H), 7.63–7.71 (m, 2H), 7.88 (m, 1H), 8.27 (s, 1H), 8.68 (s, 1H), 11.97 (brd d, 1H, NH), 13.04 (brd d, 1H, NH). MS (ESI+) m/z : 404. Anal. calcd. For $\text{C}_{17}\text{H}_{14}\text{BrN}_3\text{O}_2\text{S}\cdot \text{H}_2\text{O}$: C, 48.35; H, 3.82; N, 9.95; S, 7.59 and found C, 48.16; H, 3.86; N, 9.68; S, 7.45.

2.1.3.3. 5-(ethylsulfonyl)-2-(1H-indol-3-yl)-1-methyl-1H-benzo[d]imidazole (25). Compound **25** was prepared according to general methods starting from N^1 -methyl-4-ethylsulfonyl-benzene-1,2-diamine (0.99 mmol, 0.211 g) and indole-3-carboxaldehyde (0.99 mmol, 0.143 g). The residue was purified by cc using the ethyl acetate/hexane (1:1) as

eluent to give a white solid, m.p. 273 °C (0.095 g, 28% yield). ^1H NMR (400 MHz, $\text{DMSO}-d_6$): δ ppm 1.11 (t, 3H), 3.31 (q, 2H), 4.06 (s, 3H), 7.19–7.28 (m, 2H), 7.54 (d, $J = 7.6$ Hz, 1H), 7.72 (dd, $J = 8.4$ Hz, $J = 2$ Hz, 1H), 7.84 (d, $J = 8.4$ Hz, 1H), 8.13 (d, $J = 1.6$ Hz, 1H), 8.20 (d, $J = 2.8$ Hz, 1H), 8.44 (d, $J = 7.6$ Hz, 1H), 11.93 (brd s, 1H, NH). ^{13}C NMR ($\text{DMSO}-d_6$): 7.43, 32.01, 49.77, 104.33, 110.39, 111.81, 118.21, 120.52, 120.61, 121.53, 122.54, 126.29, 127.76, 131.26, 136.08, 139.35, 142.54, 152.90. MS (ESI+) m/z : 340. Anal. calcd. For $\text{C}_{18}\text{H}_{17}\text{N}_3\text{O}_2\text{S}\cdot 0.3\text{H}_2\text{O}$: C, 62.69; H, 5.14; N, 12.18; S, 9.29 and found C, 62.57; H, 5.06; N, 12.21; S, 9.08.

2.1.3.4. 5-(ethylsulfonyl)-2-(5-methoxy-1H-indol-3-yl)-1-methyl-1H-benzo[d]imidazole (26). Compound **26** was prepared according to general methods starting from N^1 -methyl-4-ethylsulfonyl-benzene-1,2-diamine (0.92 mmol, 0.2197 g) and 5-methoxy-indole-3-carboxaldehyde (0.92 mmol, 0.161 g). The residue was purified by cc using the ethyl acetate/hexane (1:1) as eluent to give a light yellow solid, m.p. 198 °C (0.125 g, 37% yield). ^1H NMR (400 MHz, $\text{DMSO}-d_6$): δ ppm 1.11 (t, 3H), 3.30 (q, 2H), 3.82 (s, 3H), 4.05 (s, 3H), 6.90 (dd, $J = 8.8$ Hz, $J = 2$ Hz, 1H), 7.43 (d, $J = 8.8$ Hz, 1H), 7.71 (dd, $J = 8.4$ Hz, $J = 2$ Hz, 1H), 7.82 (d, $J = 8.4$ Hz, 1H), 7.97 (d, $J = 2.4$ Hz, 1H), 8.14 (d, $J = 2$ Hz, 1H), 8.15 (s, 1H), 11.80 (brd s, 1H, NH). ^{13}C NMR ($\text{DMSO}-d_6$): 7.44, 32.03, 49.77, 55.38, 103.24, 104.10, 110.30, 112.55, 112.69, 118.21, 120.55, 126.93, 128.08, 131.13, 131.19, 139.33, 142.53, 153.07, 154.53. MS (ESI+) m/z : 370. Anal. calcd. For $\text{C}_{19}\text{H}_{19}\text{N}_3\text{O}_3\text{S}$: C, 61.77; H, 5.18; N, 11.37; S, 8.67 and found C, 61.21; H, 5.43; N, 11.52; S, 8.63.

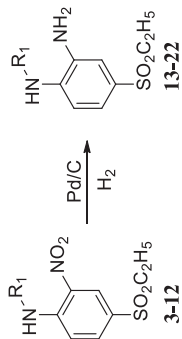
2.1.3.5. 2-(5-chloro-1H-indol-3-yl)-5-(ethylsulfonyl)-1-methyl-1H-benzo[d]imidazole (27). Compound **27** was prepared according to general methods starting from N^1 -methyl-4-ethylsulfonyl-benzene-1,2-diamine (1.15 mmol, 0.247 g) and 5-chloro-indole-3-carboxaldehyde (1.15 mmol, 0.206 g). The residue was purified by cc using the ethyl acetate/hexane (1:2) as eluent to give a light yellow solid, m.p. 264 °C (0.098 g, 23% yield). ^1H NMR (400 MHz, $\text{DMSO}-d_6$): δ ppm 1.11 (t, 3H), 3.32 (q, 2H), 4.07 (s, 3H), 7.26 (dd, $J = 8.8$ Hz, $J = 2.4$ Hz, 1H), 7.56 (d, $J = 8.4$ Hz, 1H), 7.72 (dd, $J = 8.4$ Hz, $J = 2$ Hz, 1H), 7.85 (d, $J = 8.8$ Hz, 1H), 8.17 (d, $J = 1.6$ Hz, 1H), 8.30 (s, 1H), 8.50 (d, $J = 2$ Hz, 1H). ^{13}C NMR ($\text{DMSO}-d_6$): 7.44, 32.02, 49.70, 104.08, 110.42, 113.58, 118.33, 120.69, 120.71, 122.53, 125.20, 127.47, 129.35, 131.37, 134.74, 139.27, 142.41, 152.34. MS (ESI+) m/z : 374. Anal. calcd. For $\text{C}_{18}\text{H}_{16}\text{ClN}_3\text{O}_2\text{S}\cdot 0.4\text{H}_2\text{O}$: C, 56.73; H, 4.44; N, 11.02; S, 8.41; Found: C, 56.48; H, 4.38; N, 11.02; S, 8.26.

2.1.3.6. 2-(5-bromo-1H-indol-3-yl)-5-(ethylsulfonyl)-1-methyl-1H-benzo[d]imidazole (28). Compound **28** was prepared according to general methods starting from N^1 -methyl-4-ethylsulfonyl-benzene-1,2-diamine (1.65 mmol, 0.228 g) and 5-bromo-indole-3-carboxaldehyde (1.65 mmol, 0.238 g). The residue was purified by cc using the ethyl acetate/hexane (1:1) as eluent to give a light yellow solid, m.p. 259 °C (0.052 g, 8% yield). ^1H NMR (400 MHz, $\text{DMSO}-d_6$): δ ppm 1.11 (t, 3H), 3.31 (q, 2H), 4.06 (s, 3H), 7.35 (d, $J = 8.4$ Hz, 1H), 7.54 (d, $J = 8$ Hz, 1H), 7.71 (d, $J = 8.8$ Hz, 1H), 7.83 (d, $J = 8.4$ Hz, 1H), 8.17 (s, 1H), 8.26 (s, 1H), 8.64 (s, 1H). ^{13}C NMR ($\text{DMSO}-d_6$): 7.54, 31.96, 49.72, 103.76, 110.30, 113.05, 114.14, 118.22, 120.59, 123.60, 124.81, 128.16, 129.38, 131.35, 135.22, 139.24, 142.43, 152.42. MS (ESI+) m/z : 418. Anal. calcd. For $\text{C}_{18}\text{H}_{16}\text{BrN}_3\text{O}_2\text{S}\cdot 0.35\text{H}_2\text{O}$: C, 50.91; H, 3.96; N, 9.89; S, 7.55; Found: C, 50.85; H, 3.94; N, 10.27; S, 7.45.

2.1.3.7. 1-ethyl-5-(ethylsulfonyl)-2-(1H-indol-3-yl)-1H-benzo[d]imidazole (29). Compound **29** was prepared according to general methods starting from N^1 -ethyl-4-ethylsulfonyl-benzene-1,2-diamine (1 mmol, 0.240 g) and indole-3-carboxaldehyde (1 mmol, 0.152 g). The residue was purified by cc using the ethyl acetate/metanol (4:0.5) as eluent to give a white solid, m.p. 254 °C (0.130 g, 37% yield). ^1H NMR (400 MHz, $\text{DMSO}-d_6$): δ ppm 1.13 (t, 3H), 1.42 (t, 3H), 3.32 (q, 2H), 4.56 (q, 2H), 7.19–7.28 (m, 2H), 7.54 (d, $J = 8$ Hz, 1H), 7.73 (dd, $J = 8.4$ Hz,

Table 1
Physicochemical data for compounds 3–22.

Comp.	R ₁	¹ H NMR	M.p. (°C)	Yield %	Comp.	Mass
3	-H	1.29 (t, 3H), 3.11 (q, 2H), 6.96 (d, J = 9.2 Hz, 1H), 7.77 (dd, J = 9.2 Hz, J = 2 Hz, 1H), 8.68 (d, J = 2 Hz, 1H).	143	88	13	201
4	-CH ₃	1.12 (t, 3H), 3.03 (d, 3H), 3.28 (q, 2H), 7.18 (d, J = 8.8 Hz, 1H), 7.89 (dd, J = 9 Hz, J = 2.4 Hz, 1H), 8.45 (d, J = 2 Hz, 1H), 8.68 (d, 1H, NH).	138	83	14	215
5	-C ₂ H ₅	1.09 (t, 3H), 1.2 (t, 3H), 1.64 (m, 2H), 3.25 (q, 2H), 3.46 (m, 2H), 7.22 (d, J = 8.8 Hz, 1H), 7.83 (dd, J = 9.2 Hz, J = 2.4 Hz, 1H), 8.42 (d, J = 1.6 Hz, 1H), 8.59 (t, 1H, NH).	125	84	15	229
6	-C ₆ H ₇	0.94 (t, 3H), 1.12 (t, 3H), 1.64 (m, 2H), 3.28 (q, 2H), 3.40 (q, 2H), 7.25 (d, J = 9.2 Hz, 1H), 7.84 (dd, J = 9.2 Hz, J = 2.4 Hz, 1H), 8.44 (d, J = 2.4 Hz, 1H), 8.61 (t, 1H, NH).	90	81	16	243
7	-C ₄ H ₉	0.92 (t, 3H), 1.11 (t, 3H), 1.38 (m, 2H), 1.61 (m, 2H), 3.26 (q, 2H), 3.44 (q, 2H), 7.25 (d, J = 8.8 Hz, 1H), 7.85 (dd, J = 8.8 Hz, J = 2 Hz, 1H), 8.44 (d, J = 2 Hz, 1H), 8.60 (t, 1H, NH).	76	82	17	257
8	-cyclohexyl	1.11 (t, 3H), 1.26 (m, 1H), 1.43 (m, 4H), 1.61 (d, 1H), 1.71 (m, 2H), 1.95 (m, 2H), 3.27 (q, 2H), 3.75 (m, 1H), 7.34 (d, J = 9.6 Hz, 1H), 7.85 (dd, J = 9.2 Hz, J = 2.4 Hz, 1H), 8.32 (d, J = 8 Hz, 1H), 8.55 (d, J = 2.4 Hz, 1H).	154	80	18	283
9	-benzyl	1.09 (t, 3H), 3.25 (q, 2H), 4.72 (d, 2H), 7.10 (d, J = 9.2 Hz, 1H), 7.30 (m, 5H), 7.79 (dd, J = 9.4 Hz, J = 2.4 Hz, 1H), 8.47 (d, J = 2 Hz, 1H), 9.18 (t, 1H, NH).	120	75	19	291
10	-p-fluorobenzyl	1.08 (t, 3H), 3.26 (q, 2H), 4.70 (d, 2H), 7.09 (d, J = 9.2 Hz, 1H), 7.17 (m, 2H), 7.43 (m, 2H), 7.79 (dd, J = 9.2 Hz, J = 1.6 Hz, 1H), 8.46 (d, J = 2.4 Hz, 1H), 9.19 (t, 1H, NH).	114	73	20	309
11	-3,4-difluorobenzyl	1.08 (t, 3H), 3.26 (q, 2H), 4.70 (d, 2H), 7.07 (d, J = 9.2 Hz, 1H), 7.25 (m, 1H), 7.37–7.52 (m, 2H), 7.79 (dd, J = 9.2 Hz, J = 2 Hz, 1H), 8.46 (d, J = 2.4 Hz, 1H), 9.20 (t, 1H, NH).	121	71	21	357
12	-3,4-dichlorobenzyl	1.28 (t, 3H), 3.09 (q, 2H), 4.58 (d, 2H), 6.85 (d, J = 8.8 Hz, 1H), 7.18 (dd, J = 8 Hz, J = 1.2 Hz, 1H), 7.43 (m, 2H), 7.80 (dd, J = 9 Hz, J = 2 Hz, 1H), 8.73 (d, J = 2 Hz, 1H), 8.79 (t, 1H, NH).	145	76	22	390



$J = 1.6$ Hz, 1H), 7.86 (d, $J = 8.8$ Hz, 1H), 8.09 (d, $J = 1.6$ Hz, 1H), 8.15 (d, $J = 1.6$ Hz, 1H), 8.40 (d, $J = 8$ Hz, 1H), 11.90 (brd s, 1H, NH). ^{13}C NMR (DMSO- d_6): 7.36, 14.61, 49.69, 104.04, 110.39, 111.79, 118.30, 120.43, 120.70, 121.44, 122.46, 126.35, 126.73, 131.40, 136.04, 138.33, 142.65, 151.89. MS (ESI+) m/z : 354. Anal. calcd. For $\text{C}_{19}\text{H}_{19}\text{N}_3\text{O}_2\text{S}$: C, 64.57; H, 5.41; N, 11.88; S, 9.07; Found: C, 64.67; H, 5.14; N, 11.57; S, 8.84.

2.1.3.8. 1-ethyl-5-(ethylsulfonyl)-2-(5-methoxy-1H-indol-3-yl)-1H-benzo[d]imidazole (30). Compound 30 was prepared according to general methods starting from N^1 -ethyl-4-ethylsulfonyl-benzene-1,2-diamine (1.22 mmol, 0.280 g) and 5-methoxy-indole-3-carboxaldehyde (1.22 mmol, 0.214 g). The residue was purified by cc using the ethyl acetate as eluent to give a light yellow solid, m.p. 249 °C (0.165 g, 36% yield). ^1H NMR (400 MHz, DMSO- d_6): δ ppm 1.12 (t, 3H), 1.41 (t, 3H), 3.30 (q, 2H), 3.82 (s, 3H), 4.55 (q, 2H), 6.90 (dd, $J = 8.8$ Hz, $J = 2.4$ Hz, 1H), 7.43 (d, $J = 8.8$ Hz, 1H), 7.71 (dd, $J = 8.8$ Hz, $J = 1.6$ Hz, 1H), 7.85 (d, $J = 8.8$ Hz, 1H), 7.95 (d, $J = 2.4$ Hz, 1H), 8.04 (d, $J = 3.2$ Hz, 1H), 8.15 (d, $J = 1.6$ Hz, 1H), 11.76 (brd d, 1H, NH). ^{13}C NMR (DMSO- d_6): 7.43, 14.66, 49.76, 55.35, 103.19, 103.87, 110.37, 112.57, 112.72, 118.36, 120.71, 127.05, 127.13, 131.14, 131.41, 138.39, 142.69, 152.13, 154.52. MS (ESI+) m/z : 384. Anal. calcd. For $\text{C}_{20}\text{H}_{21}\text{N}_3\text{O}_3\text{S}$: C, 60.10; H, 5.74; N, 10.51; S, 8.02; Found: C, 60.05; H, 5.75; N, 10.12; S, 7.85;

2.1.3.9. 2-(5-chloro-1H-indol-3-yl)-1-ethyl-5-(ethylsulfonyl)-1H-benzo[d]imidazole (31). Compound 31 was prepared according to general methods starting from N^1 -ethyl-4-ethylsulfonyl-benzene-1,2-diamine (1.5 mmol, 0.342 g) and 5-chloro-indole-3-carboxaldehyde (1.5 mmol, 0.269 g). The residue was purified by cc using the ethyl acetate as eluent to give a light yellow solid, m.p. 280 °C (0.273 g, 47% yield). ^1H NMR (400 MHz, DMSO- d_6): δ ppm 1.10 (t, 3H), 1.40 (t, 3H), 3.29 (q, 2H), 4.55 (q, 2H), 7.25 (dd, $J = 8.8$ Hz, $J = 2$ Hz, 1H), 7.54 (d, $J = 7.6$ Hz, 1H), 7.71 (dd, $J = 8.4$ Hz, $J = 1.6$ Hz, 1H), 7.84 (d, $J = 8$ Hz, 1H), 8.17 (t, 2H), 8.47 (d, $J = 2$ Hz, 1H), 12.07 (brd s, 1H, NH). ^{13}C NMR (DMSO- d_6): 7.41, 14.63, 49.69, 103.92, 110.46, 113.50, 118.51, 120.79, 120.88, 122.62, 125.28, 127.57, 128.29, 131.62, 134.63, 138.34, 142.57, 151.31. MS (ESI+) m/z : 388. Anal. calcd. For $\text{C}_{19}\text{H}_{18}\text{ClN}_3\text{O}_2\text{S}$: C, 58.83; H, 4.67; N, 10.83; S, 8.26; Found: C, 58.56; H, 4.67; N, 10.64; S, 8.13.

2.1.3.10. 2-(5-bromo-1H-indol-3-yl)-1-ethyl-5-(ethylsulfonyl)-1H-benzo[d]imidazole (32). Compound 32 was prepared according to general methods starting from N^1 -ethyl-4-ethylsulfonylbenzene-1,2-diamine (1.8 mmol, 0.406 g) and 5-bromo-indole-3-carboxaldehyde (1.8 mmol, 0.401 g). The residue was purified by cc using the ethyl acetate as eluent to give a light yellow solid, m.p. 288 °C (0.370 g, 48% yield). ^1H NMR (400 MHz, DMSO- d_6): δ ppm 1.10 (t, 3H), 1.40 (t, 3H), 3.29 (q, 2H), 4.55 (q, 2H), 7.36 (dd, $J = 8.8$ Hz, $J = 2$ Hz, 1H), 7.50 (d, $J = 9.2$ Hz, 1H), 7.71 (dd, $J = 8.4$ Hz, $J = 1.6$ Hz, 1H), 7.84 (d, $J = 8.4$ Hz, 1H), 8.17 (t, 2H), 8.62 (d, $J = 2$ Hz, 1H), 12.08 (brd s, 1H, NH). ^{13}C NMR (DMSO- d_6): 7.36, 14.57, 49.63, 103.74, 110.40, 113.23, 113.89, 118.47, 120.84, 123.74, 125.10, 128.06, 128.14, 131.57, 134.81, 138.28, 142.50, 151.22. MS (ESI+) m/z : 434. Anal. calcd. For $\text{C}_{19}\text{H}_{18}\text{BrN}_3\text{O}_2\text{S}$: C, 52.78; H, 4.19; N, 9.71; S, 7.41; Found: C, 52.48; H, 3.98; N, 9.58; S, 7.39.

2.1.3.11. 5-(ethylsulfonyl)-2-(1H-indol-3-yl)-1-propyl-1H-benzo[d]imidazole (33). Compound 33 was prepared according to general methods starting from N^1 -(propyl)-4-ethylsulfonyl-benzene-1,2-diamine (1.04 mmol, 0.253 g) and indole-3-carboxaldehyde (1.04 mmol, 0.152 g). The residue was purified by cc using the chloroform/ethyl acetate/hexane (2:1:1) as eluent to give a white solid, m.p. 182 °C (0.199 g, 52% yield). ^1H NMR (400 MHz, DMSO- d_6): δ ppm 0.89 (t, 3H), 1.13 (t, 3H), 1.78–1.84 (m, 2H), 3.32 (q, 2H), 4.49 (t, 2H), 7.18–7.27 (m, 2H), 7.53–7.55 (m, 1H), 7.72 (dd,

$J = 8.4$ Hz, $J = 1.6$ Hz, 1H), 7.78 (d, $J = 8.8$ Hz, 1H), 8.07 (s, 1H), 8.14 (d, $J = 1.6$ Hz, 1H), 8.39 (m, 1H), 11.85 (brd s, 1H). ^{13}C NMR (DMSO- d_6): 7.40, 10.92, 22.36, 45.57, 49.74, 104.24, 110.73, 111.85, 118.37, 120.48, 120.71, 121.46, 122.49, 126.45, 126.75, 131.43, 136.05, 138.91, 142.55, 152.20. MS (ESI+) m/z : 368. Anal. calcd. For $\text{C}_{20}\text{H}_{21}\text{N}_3\text{O}_2\text{S}$: C, 65.22; H, 6.03; N, 11.54; S, 8.68; Found: C, 65.37; H, 5.76; N, 11.44; S, 8.72.

2.1.3.12. 5-(ethylsulfonyl)-2-(5-methoxy-1H-indol-3-yl)-1-propyl-1H-benzo[d]imidazole (34). Compound 34 was prepared according to general methods starting from N^1 -(propyl)-4-ethylsulfonyl-benzene-1,2-diamine (1.06 mmol, 0.258 g) and 5-methoxy-indole-3-carboxaldehyde (1.06 mmol, 0.187 g). The residue was purified by cc using the chloroform/ethyl acetate/hexane (2:1:1) as eluent to give a white solid, m.p. 159 °C (0.175 g, 41% yield). ^1H NMR (400 MHz, DMSO- d_6): δ ppm 0.90 (t, 3H), 1.13 (t, 3H), 1.79–1.84 (m, 2H), 3.32 (q, 2H), 3.82 (s, 3H), 4.48 (t, 2H), 6.90 (dd, $J = 8.4$ Hz, $J = 2.4$ Hz, 1H), 7.44 (d, $J = 8.4$ Hz, 1H), 7.71 (dd, $J = 8.8$ Hz, $J = 1.6$ Hz, 1H), 7.87 (d, $J = 8.8$ Hz, 1H), 7.95 (d, $J = 2.4$ Hz, 1H), 8.02 (d, $J = 2.8$ Hz, 1H), 8.15 (d, $J = 2$ Hz, 1H) 11.8 (brd s, 1H) ^{13}C NMR (DMSO- d_6): 7.40, 10.93, 22.34, 45.57, 49.73, 55.35, 103.20, 103.99, 110.62, 112.55, 112.67, 118.35, 120.66, 127.08, 131.08, 131.36, 138.91, 142.51, 152.36, 154.51. MS (ESI+) m/z : 398. Anal. calcd. For $\text{C}_{21}\text{H}_{23}\text{N}_3\text{O}_3\text{S}$: C, 63.46; H, 5.83; N, 10.57; S, 8.07; Found: C, 63.18; H, 5.99; N, 10.50; S, 7.93.

2.1.3.13. 5-(ethylsulfonyl)-2-(5-chloro-1H-indol-3-yl)-1-propyl-1H-benzo[d]imidazole (35). Compound 35 was prepared according to general methods starting from N^1 -(propyl)-4-ethylsulfonyl-benzene-1,2-diamine (0.82 mmol, 0.199 g) and 5-chloro-indole-3-carboxaldehyde (0.82 mmol, 0.147 g). The residue was purified by cc using the chloroform/ethyl acetate/hexane (2:1:1) as eluent to give a white solid, m.p. 232 °C (0.050 g, 15% yield). ^1H NMR (400 MHz, DMSO- d_6): δ ppm 0.88 (t, 3H), 1.10 (t, 3H), 1.76–1.82 (m, 2H), 3.30 (q, 2H), 4.48 (t, 2H), 7.24 (dd, $J = 8.8$ Hz, $J = 2$ Hz, 1H), 7.54 (d, $J = 8.8$ Hz, 1H), 7.70 (dd, $J = 8.8$ Hz, $J = 1.6$ Hz, 1H), 7.86 (d, $J = 8.4$ Hz, 1H), 8.15–8.17 (m, 2H), 8.46 (d, $J = 2$ Hz, 1H), 12.03 (brd s, 1H). ^{13}C NMR (DMSO- d_6): 7.34, 10.87, 22.30, 45.48, 49.60, 103.97, 110.69, 113.45, 118.46, 120.71, 120.78, 122.54, 125.20, 127.56, 128.19, 131.50, 134.51, 138.82, 142.34, 151.49. MS (ESI+) m/z : 402. Anal. calcd. For $\text{C}_{20}\text{H}_{20}\text{ClN}_3\text{O}_2\text{S}$: C, 59.77; H, 5.02; N, 10.46; S, 7.98; Found: C, 59.85; H, 5.20; N, 10.54; S, 7.77.

2.1.3.14. 5-(ethylsulfonyl)-2-(5-bromo-1H-indol-3-yl)-1-propyl-1H-benzo[d]imidazole (36). Compound 36 was prepared according to general methods starting from N^1 -(propyl)-4-ethylsulfonyl-benzene-1,2-diamine (1.11 mmol, 0.269 g) and 5-bromo-indole-3-carboxaldehyde (1.11 mmol, 0.249 g). The residue was purified by cc using the chloroform/ethyl acetate/hexane (2:1:1) as eluent to give a white solid, m.p. 234 °C (0.079 g, 16% yield). ^1H NMR (400 MHz, DMSO- d_6): δ ppm 0.87 (t, 3H), 1.11 (t, 3H), 1.76–1.82 (m, 2H), 3.29 (q, 3H), 4.47 (t, 2H) 7.35 (d, $J = 8$ Hz, 1H), 7.49 (d, $J = 8.8$ Hz, 1H), 7.7 (d, $J = 8.4$ Hz, 1H), 7.84 (d, $J = 8.4$ Hz, 1H), 8.11 (s, 1H), 8.16 (s, 1H), 8.6 (s, 1H), 11.98 (brd s, 1H). ^{13}C NMR (DMSO- d_6): 7.39, 10.92, 22.35, 45.54, 49.66, 103.93, 110.76, 113.28, 113.95, 118.52, 120.85, 123.77, 125.14, 128.09, 128.24, 131.59, 134.81, 138.87, 142.40, 151.52. MS (ESI+) m/z : 446. Anal. calcd. For $\text{C}_{20}\text{H}_{20}\text{BrN}_3\text{O}_2\text{S}$: C, 53.81; H, 4.51; N, 9.41; S, 7.18; Found: C, 53.26; H, 4.51; N, 9.56; S, 6.98.

2.1.3.15. 5-(ethylsulfonyl)-2-(1H-indol-3-yl)-1-butyl-1H-benzo[d]imidazole (37). Compound 37 was prepared according to general methods starting from N^1 -(butyl)-4-ethylsulfonyl-benzene-1,2-diamine (0.89 mmol, 0.228 g) and indole-3-carboxaldehyde (0.89 mmol, 0.129 g). The residue was purified by cc using the chloroform/ethyl acetate/hexane (2:1:1) as eluent to give a white solid, m.p. 177 °C

(0.044 g, 13% yield). $^1\text{H NMR}$ (400 MHz, $\text{DMSO}-d_6$): δ ppm 0.82 (t, 3H), 1.10 (t, 3H), 1.29 (m, 2H), 1.71–1.75 (m, 2H), 3.30 (q, 2H), 4.50 (t, 2H), 7.15–7.24 (m, 2H), 7.51 (d, $J = 7.6$ Hz, 1H), 7.70 (dd, $J = 8.8$ Hz, $J = 1.6$ Hz, 1H), 7.85 (d, $J = 8.4$ Hz, 1H), 8.06 (d, $J = 2.4$ Hz, 1H), 8.12 (d, $J = 1.6$ Hz, 1H), 8.34 (d, $J = 8$ Hz, 1H), 11.84 (brd s, 1H). $^{13}\text{C NMR}$ ($\text{DMSO}-d_6$): 7.33, 13.42, 19.31, 31.02, 43.90, 49.65, 104.16, 110.62, 111.79, 118.31, 120.41, 120.67, 121.36, 122.43, 126.36, 126.71, 131.35, 135.96, 138.77, 142.50, 152.10. **MS** (ESI+) m/z : 382. **Anal. calcd.** For $\text{C}_{21}\text{H}_{23}\text{N}_3\text{O}_2\text{S}\cdot 0.2\text{H}_2\text{O}$: C, 65.49; H, 6.12; N, 10.91; S, 8.30; Found: C, 65.20; H, 6.11; N, 11.10; S, 8.30.

2.1.3.16. 5-(ethylsulfonyl)-2-(5-chloro-1H-indol-3-yl)-1-butyl-1H-benzo[d]imidazole (38). Compound **38** was prepared according to general methods starting from N^1 -(butyl)-4-ethylsulfonyl-benzene-1,2-diamine (1.08 mmol, 0.277 g) and 5-chloro-indole-3-carboxaldehyde (1.08 mmol, 0.194 g). The residue was purified by cc using the chloroform/ethyl acetate/hexane (2:1:1) as eluent to give a white solid, m.p. 221 °C (0.065 g, 14% yield). $^1\text{H NMR}$ (400 MHz, $\text{DMSO}-d_6$): δ ppm 0.87 (t, 3H), 1.13 (t, 3H), 1.32–1.37 (m, 2H), 1.75–1.79 (m, 2H), 3.30 (q, 2H), 4.51 (t, 2H), 7.28 (dd, $J = 8.4$ Hz, $J = 2.4$ Hz, 1H), 7.58 (d, $J = 8.4$ Hz, 1H), 7.74 (dd, $J = 8.4$ Hz, $J = 2$ Hz, 1H), 7.88 (d, $J = 8.8$ Hz, 1H), 8.2 (s, 2H), 8.48 (d, $J = 2.4$ Hz, 1H), 12.08 (brd s, 1H). $^{13}\text{C NMR}$ ($\text{DMSO}-d_6$): 7.45, 13.58, 19.44, 31.14, 44.01, 49.69, 104.05, 110.76, 113.57, 118.57, 120.78, 120.90, 122.65, 125.31, 127.63, 128.33, 131.59, 134.60, 138.84, 142.45, 151.55. **MS** (ESI+) m/z : 416. **Anal. calcd.** For $\text{C}_{21}\text{H}_{22}\text{ClN}_3\text{O}_2\text{S}$: C, 60.64; H, 5.33; N, 10.10; S, 7.71; Found: C, 60.23; H, 5.37; N, 10.38; S, 7.62.

2.1.3.17. 5-(ethylsulfonyl)-2-(5-bromo-1H-indol-3-yl)-1-butyl-1H-benzo[d]imidazole (39). Compound **39** was prepared according to general methods starting from N^1 -(butyl)-4-ethylsulfonyl-benzene-1,2-diamine (0.86 mmol, 0.220 g) and 5-bromo-indole-3-carboxaldehyde (0.86 mmol, 0.194 g). The residue was purified by cc using the chloroform/ethyl acetate/hexane (2:2:1) as eluent to give a white solid, m.p. 235 °C (0.040 g, 10% yield). $^1\text{H NMR}$ (400 MHz, $\text{DMSO}-d_6$): δ ppm 0.86 (t, 3H), 1.13 (t, 3H), 1.30–1.39 (m, 2H), 1.73–1.80 (m, 2H), 3.33 (q, 2H), 4.54 (t, 2H), 7.38 (dd, $J = 8.8$ Hz, $J = 1.6$ Hz, 1H), 7.53 (d, $J = 8.4$ Hz, 1H), 7.78 (dd, $J = 8.4$ Hz, $J = 1.6$ Hz, 1H), 7.88 (d, $J = 8.8$ Hz, 1H), 8.17 (s, 1H), 8.2 (d, $J = 1.6$ Hz, 1H), 8.62 (d, $J = 2$ Hz, 1H), 12.06 (brd s, 1H). $^{13}\text{C NMR}$ ($\text{DMSO}-d_6$): 7.40, 13.52, 19.39, 31.09, 43.98, 49.66, 103.92, 110.72, 113.28, 113.96, 118.54, 120.86, 123.73, 125.14, 128.11, 128.23, 131.59, 134.81, 138.79, 142.42, 151.48. **MS** (ESI+) m/z : 460. **Anal. calcd.** For $\text{C}_{21}\text{H}_{22}\text{BrN}_3\text{O}_2\text{S}$: C, 54.78; H, 4.81; N, 9.12; S, 6.96; Found: C, 54.28; H, 4.67; N, 9.51; S, 6.96.

2.1.3.18. 1-cyclohexyl-5-(ethylsulfonyl)-2-(1H-indol-3-yl)-1H-benzo[d]imidazole (40). Compound **40** was prepared according to general methods starting from N^1 -cyclohexyl-4-ethylsulfonyl-benzene-1,2-diamine (0.94 mmol, 0.265 g) and indole-3-carboxaldehyde (0.94 mmol, 0.136 g). The residue was purified by cc using the chloroform/ethyl acetate (1:1) as eluent to give a light yellow solid, m.p. 250 °C (0.263 g, 69% yield). $^1\text{H NMR}$ (400 MHz, $\text{DMSO}-d_6$): δ ppm 1.14 (t, 3H), 1.32–1.43 (m, 3H), 1.66 (d, 1H), 1.85–1.98 (m, 4H), 2.29–2.37 (m, 2H), 3.30 (q, 2H), 4.62–4.68 (m, 1H), 7.15–7.26 (m, 2H), 7.55 (d, $J = 8.4$ Hz, 1H), 7.68 (dd, $J = 8.8$ Hz, $J = 1.6$ Hz, 1H), 7.84 (d, $J = 2.8$ Hz, 1H), 7.97 (d, $J = 8$ Hz, 1H), 8.10 (d, $J = 8.8$ Hz, 1H), 8.14 (d, $J = 1.6$ Hz, 1H), 11.79 (brd s, 1H, NH). $^{13}\text{C NMR}$ ($\text{DMSO}-d_6$): 7.28, 24.32, 25.47, 30.49, 49.70, 56.58, 104.18, 111.96, 113.11, 118.84, 120.12, 120.29, 122.27, 126.46, 127.13, 131.29, 136.05, 136.85, 143.42, 152.21. **MS** (ESI+) m/z : 408. **Anal. calcd.** For $\text{C}_{23}\text{H}_{25}\text{N}_3\text{O}_2\text{S}\cdot 0.3\text{H}_2\text{O}$: C, 66.89; H, 6.25; N, 10.18; S, 7.74; Found: C, 66.57; H, 5.95; N, 9.94; S, 7.97.

2.1.3.19. 1-cyclohexyl-5-(ethylsulfonyl)-2-(5-methoxy-1H-indol-3-yl)-1H-

benzo[d]imidazole (41). Compound **41** was prepared according to general methods starting from N^1 -cyclohexyl-4-ethylsulfonyl-benzene-1,2-diamine (1.05 mmol, 0.297 g) and 5-methoxy-indole-3-carboxaldehyde (1.05 mmol, 0.184 g). The residue was purified by cc using the chloroform/ethyl acetate (1:1) as eluent to give a light yellow solid, m.p. 163 °C (0.061 g, 13% yield). $^1\text{H NMR}$ (400 MHz, $\text{DMSO}-d_6$): δ ppm 1.13 (t, 3H), 1.32–1.44 (m, 3H), 1.66 (d, 1H), 1.85–1.98 (m, 4H), 2.30–2.36 (m, 2H), 3.31 (q, 2H), 3.77 (s, 3H), 4.60–4.66 (m, 1H), 6.89 (dd, $J = 8.8$ Hz, $J = 2.4$ Hz, 1H), 7.45 (m, 2H), 7.67 (dd, $J = 8.8$ Hz, $J = 1.6$ Hz, 1H), 7.79 (d, $J = 2.8$ Hz, 1H), 8.09 (d, $J = 8.8$ Hz, 1H), 8.14 (d, $J = 1.6$ Hz, 1H), 11.68 (brd s, 1H, NH). $^{13}\text{C NMR}$ ($\text{DMSO}-d_6$): 7.37, 14.04, 24.38, 25.56, 30.55, 49.72, 55.24, 56.63, 59.71, 101.51, 104.01, 112.74, 112.82, 113.17, 118.88, 120.31, 126.95, 127.66, 131.10, 131.25, 136.92, 143.49, 152.45, 154.43. **MS** (ESI+) m/z : 438. **Anal. calcd.** For $\text{C}_{24}\text{H}_{27}\text{N}_3\text{O}_3\text{S}\cdot 0.9\text{H}_2\text{O}$: C, 63.52; H, 6.40; N, 9.26; S, 7.05; Found: C, 63.60; H, 6.40; N, 8.86; S, 6.81.

2.1.3.20. 2-(5-chloro-1H-indol-3-yl)-1-cyclohexyl-5-(ethylsulfonyl)-1H-benzo[d]imidazole (42). Compound **42** was prepared according to general methods starting from N^1 -cyclohexyl-4-ethylsulfonyl-benzene-1,2-diamine (1.12 mmol, 0.315 g) and 5-chloro-indole-3-carboxaldehyde (1.12 mmol, 0.200 g). The residue was purified by cc using the chloroform/ethyl acetate (2:1) as eluent to give a white solid, m.p. 182 °C (0.201 g, 41% yield). $^1\text{H NMR}$ (400 MHz, $\text{DMSO}-d_6$): δ ppm 1.14 (t, 3H), 1.38–1.43 (m, 3H), 1.67–2.00 (m, 5H), 2.30–2.35 (m, 2H), 3.33 (q, 2H), 4.63–4.69 (m, 1H), 7.26 (dd, $J = 8.8$ Hz, $J = 2$ Hz, 1H), 7.59 (d, $J = 9.2$ Hz, 1H), 7.71–7.73 (m, 1H), 7.98 (d, $J = 2$ Hz, 1H), 8.05 (d, $J = 1.6$ Hz, 1H), 8.14–8.19 (m, 2H), 12.06 (brd s, 1H, NH). $^{13}\text{C NMR}$ ($\text{DMSO}-d_6$): 7.35, 24.33, 25.43, 30.42, 49.65, 56.94, 103.06, 113.64, 113.78, 118.48, 119.64, 120.88, 122.60, 125.31, 127.56, 129.22, 131.93, 134.68, 136.47, 141.93, 151.22. **MS** (ESI+) m/z : 442. **Anal. calcd.** For $\text{C}_{23}\text{H}_{24}\text{ClN}_3\text{O}_2\text{S}$: C, 62.50; H, 5.47; N, 9.51; S, 7.25; Found: C, 62.23; H, 5.71; N, 8.94; S, 7.12.

2.1.3.21. 2-(5-bromo-1H-indol-3-yl)-1-cyclohexyl-5-(ethylsulfonyl)-1H-benzo[d]imidazole (43). Compound **43** was prepared according to general methods starting from N^1 -cyclohexyl-4-ethylsulfonyl-benzene-1,2-diamine (1.10 mmol, 0.311 g) and 5-bromo-indole-3-carboxaldehyde (1.10 mmol, 0.246 g). The residue was purified by cc using the chloroform/ethyl acetate (1:1) as eluent to give a white solid, m.p. 184 °C (0.335 g, 79% yield). $^1\text{H NMR}$ (400 MHz, $\text{DMSO}-d_6$): δ ppm 1.13 (t, 3H), 1.40 (m, 3H), 1.67 (s, 1H), 1.86–1.98 (m, 4H), 2.29–2.35 (m, 2H), 3.31 (q, 2H), 4.63–4.69 (m, 1H), 7.36 (dd, $J = 8.4$ Hz, $J = 1.6$ Hz, 1H), 7.53 (d, $J = 8.4$ Hz, 1H), 7.68 (dd, $J = 8.4$ Hz, $J = 2$ Hz, 1H), 7.93 (d, $J = 2.8$ Hz, 1H), 8.10 (d, $J = 8.8$ Hz, 1H), 8.20 (dd, $J = 11.2$ Hz, $J = 1.6$ Hz, 2H), 11.99 (brd s, 1H, NH). $^{13}\text{C NMR}$ ($\text{DMSO}-d_6$): 7.27, 24.32, 25.41, 30.45, 49.65, 56.65, 103.78, 113.05, 113.21, 114.00, 118.91, 120.40, 122.70, 124.92, 128.30, 128.40, 131.47, 134.83, 136.76, 143.23, 151.43. **MS** (ESI+) m/z : 488. **Anal. calcd.** For $\text{C}_{23}\text{H}_{24}\text{BrN}_3\text{O}_2\text{S}\cdot 0.45\text{H}_2\text{O}$: C, 55.86; H, 5.07; N, 8.49; S, 6.48; Found: C, 55.85; H, 4.85; N, 8.15; S, 6.43.

2.1.3.22. 1-benzyl-5-(ethylsulfonyl)-2-(1H-indol-3-yl)-1H-benzo[d]imidazole (44). Compound **44** was prepared according to general methods starting from N^1 -benzyl-4-ethylsulfonyl-benzene-1,2-diamine (0.80 mmol, 0.230 g) and indole-3-carboxaldehyde (0.80 mmol, 0.115 g). The residue was purified by cc using the chloroform/ethyl acetate (1:1) as eluent to give a white solid, m.p. 252 °C (0.066 g, 20% yield). $^1\text{H NMR}$ (400 MHz, $\text{DMSO}-d_6$): δ ppm 1.14 (t, 3H), 3.31 (q, 2H), 5.85 (s, 2H), 7.09 (d, $J = 7.2$ Hz, 2H), 7.19–7.34 (m, 5H), 7.49 (d, $J = 7.2$ Hz, 1H), 7.68–7.78 (m, 3H), 8.19 (s, 1H), 8.44 (d, $J = 7.2$ Hz, 1H), 11.77 (brd s, 1H, NH). $^{13}\text{C NMR}$ ($\text{DMSO}-d_6$): 7.38, 47.38, 49.68, 103.92, 110.74, 111.87, 118.48, 120.63, 121.09, 121.50, 122.63, 125.96, 126.33, 126.84, 127.48, 128.93, 131.90, 135.98, 136.57, 139.12, 142.69, 152.61. **MS** (ESI+) m/z : 416. **Anal. calcd.** For

C₂₄H₂₁N₃O₂S.0,5C₄H₈O₂.0,5H₂O: C, 66.65; H, 5.59; N, 8.97; S, 6.84; Found: C, 66.68; H, 5.40; N, 8.98; S, 6.90.

2.1.3.23. 1-benzyl-5-(ethylsulfonyl)-2-(5-methoxy-1H-indol-3-yl)-1H-benzo[d]imidazole (45). Compound 45 was prepared according to general methods starting from N¹-benzyl-4-ethylsulfonyl-benzene-1,2-diamine (0.70 mmol, 0.203 g) and 5-methoxy-indole-3-carboxaldehyde (0.70 mmol, 0.123 g). The residue was purified by cc using the chloroform/ethyl acetate (1:1) as eluent to give a white solid, m.p. 296 °C (0.036 g, 12% yield). ¹H NMR (400 MHz, DMSO-*d*₆): δ ppm 1.13 (t, 3H), 3.32 (q, 2H), 3.80 (s, 3H), 5.83 (s, 2H), 6.88 (dd, *J* = 8.8 Hz, *J* = 2.4 Hz, 1H), 7.09 (d, *J* = 7.2 Hz, 2H), 7.23–7.39 (m, 4H), 7.67–7.74 (m, 3H), 7.96 (d, *J* = 2.4 Hz, 1H), 8.19 (d, *J* = 1.2 Hz, 1H), 11.64 (brd s, 1H, NH). ¹³C NMR (DMSO-*d*₆): 7.89, 47.89, 60.18, 55.81, 103.62, 104.17, 111.15, 113.09, 113.29, 118.98, 121.52, 126.47, 127.44, 127.72, 127.96, 129.43, 131.47, 132.32, 137.08, 139.62, 143.19, 153.31, 155.07. **MS (ESI+)** *m/z*: 446. **Anal. calcd. For C₂₅H₂₃N₃O₃S**: C, 67.39; H, 5.20; N, 9.43; S, 7.19; Found: C, 67.29; H, 5.45; N, 9.30; S, 7.16.

2.1.3.24. 1-benzyl-2-(5-chloro-1H-indol-3-yl)-5-(ethylsulfonyl)-1H-benzo[d]imidazole (46). Compound 46 was prepared according to general methods starting from N¹-benzyl-4-ethylsulfonylbenzene-1,2-diamine (0.85 mmol, 0.246 g) and 5-chloro-indole-3-carboxaldehyde (0.85 mmol, 0.152 g). The residue was purified by cc using the chloroform/ethyl acetate (1:1) as eluent to give a white solid, m.p. 265 °C (0.139 g, 36% yield). ¹H NMR (400 MHz, DMSO-*d*₆): δ ppm 1.15 (t, 3H), 3.32 (q, 2H), 5.86 (s, 2H), 7.09 (d, *J* = 7.6 Hz, 2H), 7.25–7.34 (m, 4H), 7.52 (d, *J* = 8.8 Hz, 1H), 7.70–7.78 (m, 2H), 7.8 (s, 1H), 8.25 (s, 1H), 8.51 (d, *J* = 2 Hz, 1H), 11.95 (brd s, 1H, NH). ¹³C NMR (DMSO-*d*₆): 7.31, 47.33, 49.62, 103.71, 110.71, 113.48, 118.61, 120.70, 121.16, 122.66, 125.34, 125.90, 127.45, 128.24, 128.89, 132.05, 134.46, 136.38, 139.05, 142.53, 151.95. **MS (ESI+)** *m/z*: 450. **Anal. calcd. For C₂₄H₂₀ClN₃O₂S**: C, 64.06; H, 4.48; N, 9.33; S, 7.12; Found: C, 63.47; H, 4.46; N, 9.19; S, 7.05.

2.1.3.25. 1-benzyl-2-(5-bromo-1H-indol-3-yl)-5-(ethylsulfonyl)-1H-benzo[d]imidazole (47). Compound 47 was prepared according to general methods starting from N¹-benzyl-4-ethylsulfonyl-benzene-1,2-diamine (0.83 mmol, 0.240 g) and 5-bromo-indole-3-carboxaldehyde (0.83 mmol, 0.185 g). The residue was purified by cc using the chloroform/ethyl acetate (1:1) as eluent to give a white solid, m.p. 267 °C (0.226 g, 55% yield). ¹H NMR (400 MHz, DMSO-*d*₆): δ ppm 1.13 (t, 3H), 3.33 (q, 2H), 5.87 (s, 2H), 7.08 (d, *J* = 7.2 Hz, 2H), 7.25–7.38 (m, 4H), 7.48 (d, *J* = 8.8 Hz, 1H), 7.69–7.78 (m, 2H), 7.87 (s, 1H), 8.25 (s, 1H), 8.66 (d, *J* = 1.6 Hz, 1H), 11.97 (brd s, 1H, NH). ¹³C NMR (DMSO-*d*₆): 7.38, 47.34, 49.63, 103.61, 110.75, 113.41, 113.97, 118.68, 121.23, 123.77, 125.25, 125.94, 127.50, 128.10, 128.13, 128.95, 132.05, 134.73, 136.43, 139.10, 142.55, 151.95. **MS (ESI+)** *m/z*: 496. **Anal. calcd. For C₂₄H₂₀BrN₃O₂S.0,3H₂O**: C, 57.67; H, 4.15; N, 8.40; S, 6.41; Found: C, 57.66; H, 4.12; N, 8.17; S, 6.13.

2.1.3.26. 5-(ethylsulfonyl)-1-(4-fluorobenzyl)-2-(1H-indol-3-yl)-1H-benzo[d]imidazole (48). Compound 48 was prepared according to general methods starting from N¹-(4-fluorobenzyl)-4-ethylsulfonyl-benzene-1,2-diamine (0.68 mmol, 0.210 g) and indole-3-carboxaldehyde (0.68 mmol, 0.099 g). The residue was purified by cc using the chloroform/ethyl acetate (2:1) as eluent to give a white solid, m.p. 234 °C (0.080 g, 27% yield). ¹H NMR (400 MHz, DMSO-*d*₆): δ ppm 1.13 (t, 3H), 3.31 (q, 2H), 5.82 (s, 2H), 7.08–7.24 (m, 6H), 7.48 (d, *J* = 7.2 Hz, 1H), 7.69 (dd, *J* = 8.4 Hz, *J* = 1.6 Hz, 1H), 7.71 (d, *J* = 8.8 Hz, 1H), 7.80 (d, *J* = 2.4 Hz, 1H), 8.17 (d, *J* = 1.2 Hz, 1H), 8.41 (d, *J* = 8.4 Hz, 1H), 11.73 (brd s, 1H, NH). ¹³C NMR (DMSO-*d*₆): 7.31, 46.68, 49.62, 103.80, 110.66, 111.82, 115.69 (d, *J* = 21.3 Hz), 118.46, 120.57, 121.07, 121.45, 122.57, 126.26, 126.81, 128.04 (d, *J* = 8.4 Hz), 131.90, 132.65 (d, *J* = 3.1 Hz), 135.94, 138.95, 142.66,

152.47, 161.32 (d, *J* = 242.3 Hz), 170.23. **MS (ESI+)** *m/z*: 434. **Anal. calcd. For C₂₄H₂₀FN₃O₂S.0,5C₄H₈O₂**: C, 65.39; H, 5.06; N, 8.79; S, 6.71; Found: C, 65.18; H, 5.02; N, 8.71; S, 6.68.

2.1.3.27. 5-(ethylsulfonyl)-1-(4-fluorobenzyl)-2-(5-methoxy-1H-indol-3-yl)-1H-benzo[d]imidazole (49). Compound 49 was prepared according to general methods starting from N¹-(4-fluorobenzyl)-4-ethylsulfonyl-benzene-1,2-diamine (0.54 mmol, 0.168 g) and 5-methoxy-indole-3-carboxaldehyde (0.54 mmol, 0.095 g). The residue was purified by cc using the chloroform/ethyl acetate (2:1) as eluent to give a light yellow solid, m.p. 260 °C (0.044 g, 18% yield). ¹H NMR (400 MHz, DMSO-*d*₆): δ ppm 1.13 (t, 3H), 3.32 (q, 2H), 3.80 (s, 3H), 5.82 (s, 2H), 6.89 (dd, *J* = 8.8 Hz, *J* = 2.4 Hz, 1H), 7.10–7.18 (m, 4H), 7.39 (d, *J* = 8.8 Hz, 1H), 7.67–7.77 (m, 3H), 7.96 (d, *J* = 2.4 Hz, 1H), 8.19 (d, *J* = 1.6 Hz, 1H), 11.66 (brd s, 1H, NH). ¹³C NMR (DMSO-*d*₆): 7.31, 46.68, 49.60, 55.24, 103.08, 103.55, 110.55, 112.53, 112.72, 115.68 (d, *J* = 21.7 Hz), 118.43, 120.98, 126.87, 127.16, 128.03 (d, *J* = 8.4 Hz), 130.92, 131.84, 132.64 (d, *J* = 3.5 Hz), 138.93, 142.64, 152.64, 154.51, 161.30 (d, *J* = 242.3 Hz). **MS (ESI+)** *m/z*: 464. **Anal. calcd. For C₂₅H₂₂FN₃O₃S.0,2H₂O**: C, 64.27; H, 4.83; N, 9.00; S, 6.85; Found: C, 64.02; H, 4.98; N, 8.69; S, 6.62.

2.1.3.28. 2-(5-chloro-1H-indol-3-yl)-5-(ethylsulfonyl)-1-(4-fluorobenzyl)-1H-benzo[d]imidazole (50). Compound 50 was prepared according to general methods starting from N¹-(4-fluorobenzyl)-4-ethylsulfonyl-benzene-1,2-diamine (0.52 mmol, 0.162 g) and 5-chloro-indole-3-carboxaldehyde (0.52 mmol, 0.094 g). The residue was purified by cc using the chloroform/ethyl acetate (2:1) as eluent to give a white solid, m.p. 230 °C (0.097 g, 40% yield). ¹H NMR (400 MHz, DMSO-*d*₆): δ ppm 1.12 (t, 3H), 3.32 (q, 2H), 5.83 (s, 2H), 7.08–7.15 (m, 4H), 7.24 (dd, *J* = 8.8 Hz, *J* = 2 Hz, 1H), 7.50 (d, *J* = 8.4 Hz, 1H), 7.69 (dd, *J* = 8.4 Hz, *J* = 2 Hz, 1H), 7.76 (d, *J* = 8.4 Hz, 1H), 7.9 (s, 1H), 8.22 (d, *J* = 1.6 Hz, 1H), 8.48 (d, *J* = 2.4 Hz, 1H), 11.96 (brd s, 1H, NH). ¹³C NMR (DMSO-*d*₆): 7.31, 46.44, 49.55, 103.61, 110.68, 113.49, 115.72 (d, *J* = 21.1 Hz), 118.62, 120.69, 121.20, 122.66, 125.33, 127.41, 128.03 (d, *J* = 7.7 Hz), 128.28, 132.04, 132.52 (d, *J* = 2.6 Hz), 134.43, 138.92, 142.51, 151.82, 161.32 (d, *J* = 240 Hz). **MS (ESI+)** *m/z*: 468. **Anal. calcd. For C₂₄H₁₉ClFN₃O₂S**: C, 61.60; H, 4.09; N, 8.98; S, 6.85; Found: C, 61.51; H, 4.10; N, 9.00; S, 6.86.

2.1.3.29. 2-(5-bromo-1H-indol-3-yl)-5-(ethylsulfonyl)-1-(4-fluorobenzyl)-1H-benzo[d]imidazole (51). Compound 51 was prepared according to general methods starting from N¹-(4-fluorobenzyl)-4-ethylsulfonyl-benzene-1,2-diamine (0.66 mmol, 0.202 g) and 5-bromo-indole-3-carboxaldehyde (0.66 mmol, 0.146 g). The residue was purified by cc using the chloroform/ethyl acetate/hexane (2:1:1) as eluent to give a white solid, m.p. 240 °C (0.099 g, 29% yield). ¹H NMR (400 MHz, DMSO-*d*₆): δ ppm 1.13 (t, 3H), 3.32 (q, 2H), 5.86 (s, 2H), 7.10–7.18 (m, 4H), 7.38 (dd, *J* = 8.8 Hz, *J* = 2 Hz, 1H), 7.48 (d, *J* = 8.4 Hz, 1H), 7.71 (dd, *J* = 8.4 Hz, *J* = 1.6 Hz, 1H), 7.78 (d, *J* = 8.4 Hz, 1H), 7.91 (d, *J* = 2.8 Hz, 1H), 8.25 (d, *J* = 1.6 Hz, 1H), 8.66 (d, *J* = 2 Hz, 1H), 11.99 (brd s, 1H, NH). ¹³C NMR (DMSO-*d*₆): 7.31, 46.64, 49.64, 103.49, 110.68, 113.34, 113.92, 115.72 (d, *J* = 21.2 Hz), 118.63, 121.20, 123.70, 125.20, 127.97, 128.02 (d, *J* = 8.3 Hz), 128.113, 132.05, 132.51 (d, *J* = 3.2 Hz), 134.67, 138.91, 142.50, 151.79, 161.32 (d, *J* = 241.5 Hz). **MS (ESI+)** *m/z*: 514. **Anal. calcd. For C₂₄H₁₉BrFN₃O₂S**: C, 56.26; H, 3.74; N, 8.20; S, 6.25; Found: C, 56.51; H, 4.02; N, 7.72; S, 5.84.

2.1.3.30. 5-(ethylsulfonyl)-1-(3,4-difluorobenzyl)-2-(1H-indol-3-yl)-1H-benzo[d]imidazole (52). Compound 52 was prepared according to general methods starting from N¹-(3,4-difluorobenzyl)-4-ethylsulfonyl-benzene-1,2-diamine (0.64 mmol, 0.209 g) and indole-3-carboxaldehyde (0.64 mmol, 0.093 g). The residue was purified by cc using the chloroform/ethyl acetate/hexane (2:1.5:1) as eluent to give a white solid, m.p. 262 °C (0.175 g, 61% yield). ¹H NMR (400 MHz,

DMSO-*d*₆): δ ppm 1.11 (t, 3H), 3.31 (q, 2H), 5.82 (s, 2H), 6.77 (d, $J = 8.4$ Hz, 1H), 7.16–7.36 (m, 4H), 7.48 (d, $J = 7.6$ Hz, 1H), 7.69 (dd, $J = 8.8$ Hz, $J = 1.6$ Hz, 1H), 7.75 (d, $J = 8.4$ Hz, 1H), 7.80 (d, $J = 2.8$ Hz, 1H), 8.18 (d, $J = 1.6$ Hz, 1H), 8.41 (d, $J = 8.4$ Hz, 1H), 11.77 (brd s, 1H). **MS (ESI+)** m/z : 452. **Anal. calcd. For C₂₄H₁₉F₂N₃O₂S**: C, 63.85; H, 4.24; N, 8.42; S, 7.10; Found: C, 63.61; H, 4.41; N, 8.97; S, 6.91

2.1.3.31. 5-(ethylsulfonyl)-1-(3,4-difluorobenzyl)-2-(5-methoxy-1H-indol-3-yl)-1H-benzod[imidazole (53). Compound **53** was prepared according to general methods starting from N¹-(3,4-difluorobenzyl)-4-ethylsulfonyl-benzene-1,2-diamine (0.71 mmol, 0.233 g) and 5-methoxy-indole-3-carboxaldehyde (0.71 mmol, 0.125 g). The residue was purified by cc using the chloroform/ethyl acetate/hexane (2:1:1) as eluent to give a white solid, m.p. 271 °C (0.151 g, 44% yield). **¹H NMR (400 MHz, DMSO-*d*₆)**: δ ppm 1.11 (t, 3H), 3.30 (q, 2H), 3.79 (s, 3H), 5.80 (s, 2H), 6.78 (d, 1H), 6.87 (dd, $J = 9$ Hz, $J = 2.4$ Hz, 1H), 7.24–7.39 (m, 3H), 7.67–7.76 (m, 3H), 7.94 (d, 1H), 8.19 (d, $J = 1.2$ Hz, 1H), 11.65 (brd s, 1H). **MS (ESI+)** m/z : 482. **Anal. calcd. For C₂₅H₂₁F₂N₃O₃S**: C, 62.36; H, 4.40; N, 8.73; S, 6.66; Found: C, 61.94; H, 4.60; N, 8.61; S, 6.68.

2.1.3.32. 5-(ethylsulfonyl)-1-(3,4-difluorobenzyl)-2-(5-chloro-1H-indol-3-yl)-1H-benzod[imidazole (54). Compound **54** was prepared according to general methods starting from N¹-(3,4-difluorobenzyl)-4-ethylsulfonyl-benzene-1,2-diamine (0.89 mmol, 0.293 g) and 5-chloro-indole-3-carboxaldehyde (0.89 mmol, 0.160 g). The residue was purified by cc using the chloroform/ethyl acetate/hexane (2:1:1) as eluent to give a white solid, m.p. 258 °C (0.209 g, 48% yield). **¹H NMR (400 MHz, DMSO-*d*₆)**: δ ppm 1.11 (t, 3H), 3.30 (q, 2H), 5.83 (s, 2H), 6.76 (d, 1H), 7.22–7.36 (m, 3H), 7.50 (d, $J = 8.4$ Hz, 1H), 7.70 (dd, $J = 8.6$ Hz, $J = 1.6$ Hz, 1H), 7.76 (d, $J = 8.4$ Hz, 1H), 7.9 (d, $J = 1.6$ Hz, 1H), 8.23 (d, $J = 1.6$ Hz, 1H), 8.47 (d, $J = 2.4$ Hz, 1H), 11.96 (brd s, 1H). **MS (ESI+)** m/z : 486. **Anal. calcd. For C₂₄H₁₈ClF₂N₃O₂S**: C, 59.32; H, 3.73; N, 8.65; S, 6.60; Found: C, 59.01; H, 3.74; N, 8.45; S, 6.45

2.1.3.33. 5-(ethylsulfonyl)-1-(3,4-difluorobenzyl)-2-(5-bromo-1H-indol-3-yl)-1H-benzod[imidazole (55). Compound **55** was prepared according to general methods starting from N¹-(3,4-difluorobenzyl)-4-ethylsulfonyl-benzene-1,2-diamine (0.72 mmol, 0.234 g) and 5-bromo-indole-3-carboxaldehyde (0.72 mmol, 0.160 g). The residue was purified by cc using the chloroform/ethyl acetate/hexane (2:2:1) as eluent to give a white solid, m.p. 248 °C (0.141 g, 37% yield). **¹H NMR (400 MHz, DMSO-*d*₆)**: δ ppm 1.14 (t, 3H), 3.33 (q, 2H), 5.86 (s, 2H), 6.80 (d, 1H), 7.29–7.39 (m, 3H), 7.49 (d, $J = 8.8$ Hz, 1H), 7.75 (dd, $J = 8.4$ Hz, $J = 1.6$ Hz, 1H), 7.79 (d, $J = 8.8$ Hz, 1H), 7.91 (d, $J = 2.8$ Hz, 1H), 8.26 (d, $J = 1.2$ Hz, 1H), 8.65 (d, $J = 2$ Hz, 1H), 12.00 (brd s, 1H). **MS (ESI+)** m/z : 532. **Anal. calcd. For C₂₄H₁₈BrF₂N₃O₂S**: C, 54.35; H, 3.42; N, 7.92; S, 6.04; Found: C, 54.43; H, 3.20; N, 7.84; S, 6.01.

2.1.3.34. 5-(ethylsulfonyl)-1-(3,4-dichlorobenzyl)-2-(1H-indol-3-yl)-1H-benzod[imidazole (56). Compound **56** was prepared according to general methods starting from N¹-(3,4-dichlorobenzyl)-4-ethylsulfonyl-benzene-1,2-diamine (0.44 mmol, 0.158 g) and indole-3-carboxaldehyde (0.44 mmol, 0.064 g). The residue was purified by cc using the chloroform/ethyl acetate (2:1) as eluent to give a white solid, m.p. 247 °C (0.070 g, 33% yield). **¹H NMR (400 MHz, DMSO-*d*₆)**: δ ppm 1.15 (t, 3H), 3.34 (q, 2H), 5.88 (s, 2H), 6.90 (dd, $J = 8.2$ Hz, $J = 2.4$ Hz, 1H), 7.20–7.27 (m, 2H), 7.49–7.60 (m, 3H), 7.71 (dd, $J = 8.2$ Hz, $J = 2$ Hz, 1H), 7.78 (d, $J = 8.8$ Hz, 1H), 7.82 (d, $J = 2.8$ Hz, 1H), 8.21 (d, $J = 1.6$ Hz, 1H), 8.45 (d, $J = 7.2$ Hz, 1H), 11.81 (brd s, 1H). **¹³C NMR (DMSO-*d*₆)**: 7.30, 46.30, 49.61, 103.62, 110.58, 111.84, 118.52, 120.62, 121.45, 122.63, 126.04, 126.85, 128.37, 130.07, 130.80, 131.09, 131.41, 132.07, 135.95, 137.73, 138.88, 142.65,

152.43, 161.22. **MS (ESI+)** m/z : 484. **Anal. calcd. For C₂₄H₁₉Cl₂N₃O₂S·0.5 H₂O**: C, 58.42; H, 4.08; N, 8.51; S, 6.49; Found: C, 58.30; H, 4.31; N, 8.78; S, 6.04.

2.1.3.35. 5-(ethylsulfonyl)-1-(3,4-dichlorobenzyl)-2-(5-methoxy-1H-indol-3-yl)-1H-benzod[imidazole (57). Compound **57** was prepared according to general methods starting from N¹-(3,4-dichlorobenzyl)-4-ethylsulfonyl-benzene-1,2-diamine (1.01 mmol, 0.363 g) and 5-methoxy-indole-3-carboxaldehyde (1.01 mmol, 0.177 g). The residue was purified by cc using the chloroform/ethyl acetate (2:1) as eluent to give a white solid, m.p. 242 °C (0.065 g, 12% yield). **¹H NMR (400 MHz, DMSO-*d*₆)**: δ ppm 1.11 (t, 3H), 3.31 (q, 2H), 3.79 (s, 3H), 5.83 (s, 2H), 6.89 (m, 2H), 7.37 (d, $J = 8.8$ Hz, 1H), 7.46 (d, $J = 2$ Hz, 1H), 7.53 (d, $J = 8.4$ Hz, 1H), 7.67–7.76 (m, 3H), 7.95 (d, $J = 2.4$ Hz, 1H), 8.19 (d, $J = 1.6$ Hz, 1H), 11.65 (brd s, 1H). **¹³C NMR (DMSO-*d*₆)**: 7.31, 46.30, 49.61, 55.25, 103.08, 103.39, 110.50, 112.57, 112.79, 118.52, 121.15, 126.06, 126.87, 127.20, 128.37, 130.05, 130.94, 131.09, 131.40, 132.08, 137.74, 138.87, 142.64, 152.61, 154.57. **MS (ESI+)** m/z : 514. **Anal. calcd. For C₂₅H₂₁Cl₂N₃O₃S**: C, 58.37; H, 4.11; N, 8.17; S, 6.23; Found: C, 58.04; H, 4.06; N, 7.83; S, 5.98.

2.1.3.36. 5-(ethylsulfonyl)-1-(3,4-dichlorobenzyl)-2-(5-chloro-1H-indol-3-yl)-1H-benzod[imidazole (58). Compound **58** was prepared according to general methods starting from N¹-(3,4-dichlorobenzyl)-4-ethylsulfonyl-benzene-1,2-diamine (0.56 mmol, 0.202 g) and 5-chloro-indole-3-carboxaldehyde (0.56 mmol, 0.101 g). The residue was purified by cc using the chloroform/ethyl acetate (2:1) as eluent to give a white solid, m.p. 278 °C (0.045 g, 15% yield). **¹H NMR (400 MHz, DMSO-*d*₆)**: δ ppm 1.12 (t, 3H), 3.32 (q, 2H), 5.86 (s, 2H), 6.86 (dd, $J = 8.4$ Hz, $J = 2$ Hz, 1H), 7.24 (dd, $J = 8.8$ Hz, $J = 2$ Hz, 1H), 7.47–7.53 (m, 3H), 7.71 (dd, $J = 8.2$ Hz, $J = 1.6$ Hz, 1H), 7.77 (d, $J = 8.4$ Hz, 1H), 7.90 (d, $J = 3.2$ Hz, 1H), 8.24 (d, $J = 1.6$ Hz, 1H), 8.49 (d, $J = 2$ Hz, 1H), 11.96 (brd s, 1H). **¹³C NMR (DMSO-*d*₆)**: 7.31, 46.26, 49.55, 103.44, 110.61, 113.52, 118.69, 120.69, 121.35, 122.72, 125.39, 125.99, 127.39, 128.32, 128.39, 130.09, 131.11, 131.42, 132.21, 134.45, 137.60, 138.85, 142.51, 151.80. **MS (ESI+)** m/z : 518. **Anal. calcd. For C₂₄H₁₈Cl₃N₃O₂S**: C, 55.56; H, 3.50; N, 8.10; S, 6.18; Found: C, 55.19; H, 3.35; N, 7.92; S, 5.98.

2.1.3.37. 5-(ethylsulfonyl)-1-(3,4-dichlorobenzyl)-2-(5-bromo-1H-indol-3-yl)-1H-benzod[imidazole (59). Compound **59** was prepared according to general methods starting from N¹-(3,4-dichlorobenzyl)-4-ethylsulfonyl-benzene-1,2-diamine (0.78 mmol, 0.280 g) and 5-bromo-indole-3-carboxaldehyde (0.78 mmol, 0.174 g). The residue was purified by cc using the chloroform/ethyl acetate (2:1) as eluent to give a white solid, m.p. 156 °C (0.055 g, 12% yield). **¹H NMR (400 MHz, DMSO-*d*₆)**: δ ppm 1.13 (t, 3H), 3.33 (q, 2H), 5.89 (s, 2H), 6.88 (dd, $J = 8.4$ Hz, $J = 1.6$ Hz, 1H), 7.38 (dd, $J = 8.8$ Hz, $J = 2$ Hz, 1H), 7.48–7.56 (m, 3H), 7.73 (dd, $J = 8.2$ Hz, $J = 1.6$ Hz, 1H), 7.80 (d, $J = 8.8$ Hz, 1H), 7.91 (d, $J = 3.2$ Hz, 1H), 8.27 (d, $J = 0.8$ Hz, 1H), 8.66 (d, $J = 1.6$ Hz, 1H), 12.00 (brd s, 1H). **¹³C NMR (DMSO-*d*₆)**: 12.45, 47.26, 56.68, 103.65, 110.68, 113.47, 118.45, 120.69, 121.03, 122.65, 125.31, 125.87, 127.40, 127.42, 128.23, 128.88, 132.60, 134.41, 136.37, 139.00, 142.47, 151.90. **MS (ESI+)** m/z : 564. **Anal. calcd. For C₂₄H₁₈BrCl₂N₃O₂S·0.5H₂O**: C, 50.52; H, 3.35; N, 7.37; S, 5.60; Found: C, 50.14; H, 3.05; N, 7.12; S, 5.35.

2.2. Biological activity assays

2.2.1. Cytotoxic assays on human cancer lines

3-(4,5-Dimethylthiazol-2-yl)-2,5-diphenyltetrazolium Bromide (MTT) (Molecular Probes) was used to measure cell viability. Cell lines (MCF-7, MDA-MB-231 and HEPG2) were seeded onto 96-well plates with 10,000 cells/well in phenol-free media (DMEM-low-glucose, GIBCO). After 24 h, the cells were exposed to compounds listed in [Table 2](#) with different concentrations for another day. All compounds

were tested first at 0.25 μM , 2 μM , 16 μM and 40 μM doses using MCF-7 cells. At each dose, percent cell viability was calculated in relationship to the DMSO control for each concentration. Selected compounds were further studied using three different cell lines (MCF-7, MDA-MB-231, and HEPG2) at eight different concentrations to calculate IC_{50} values. Camptothecin was used as a positive control (0.25 and 2 μM) as there was a DMSO group for calibration for each drug concentration. Cells were then fixed according to the manufacturer's instructions and intensities were measured spectrophotometrically (BIO-TEK/ μQuant Universal Microplate Spectrophotometer and BIO-TEK/KC junior software (v.1.418)). Percent viability was calculated at each dose, separately, by dividing the blank subtracted average OD values of each treated sample with the blank subtracted average ODs of corresponding DMSO treated counterparts; and the resulting values were multiplied by 100 to obtain percentile viabilities. One-way ANOVA followed by multiple comparisons (MATLAB R2016a) were used to test differences in group means between the drug and DMSO control groups at each concentration. For clustering the MTT data, percentiles were divided by 100 and logarithmically transformed at base two before performing hierarchical clustering. For testing the significance of mean differences between groups from the MCF-7 four-concentration screening, raw data from each plate of compounds were statistically compared with respect to their corresponding DMSO control values at each concentration, separately. For wider dose screens, IC_{50} values for each cell line were calculated using GraphPad Prism (v. 6.05). Further statistical analyses were performed by using the viability values obtained from MCF-7 and other cell lines, to determine any relationship between the viability and R_1 or R_2 status of the derivatives. n -way ANOVA analyses with \log_2 transformed viability values (in R environment), and one-sided Wilcoxon-rank sum test and $\log\text{IC}_{50}$ (GRcalculator [46]) were performed by taking into account the triplicate values of viability scores and corresponding treatment concentrations. In GRcalculator analyses, sigmoidal fit and capping GR values below 1 were used. Additionally, two-way ANOVA with Tukey's multiple comparisons was performed to test the significance of difference between specific groups of compounds in GraphPad Prism (v. 6.05), by using cell viability values in triplicates. Principal component analysis (PCA) was used for further investigating the effect of cell line and concentration; and \log_2 transformed cell viability was used for the analysis.

2.3. Molecular docking analyses with multiple targets

$\text{ER}\alpha$ ligand-binding domain (PDB ID:1a52, resolution: 2.8 Å) file was obtained from the RCSB Protein database website [47]. Additional proteins were tested to analyze the selectivity of compounds against $\text{ER}\alpha$. These compounds were protein kinase C beta II (PDB ID:1pfq, resolution: 1.9 Å), glycogen synthase kinase 3 (PDB ID:1io9, resolution: 2.7 Å), platelet-derived growth factor receptor beta (PDB ID:3mjg, resolution: 2.3 Å), tubulin (PDB ID:1sa0, resolution: 3.58 Å) and vEGFR2 kinase domain (PDB ID:2xir, resolution:1.5 Å), respectively. Proteins were prepared with Maestro's Protein Preparation Wizard [48] and the gridbox was prepared via the Receptor Grid Generation module of Maestro [49]. Binding sites of co-ligands were used for gridbox generation. 2D builder was used to draw the ligands and same ligands were minimized and prepared with the LigPrep module [50]. Tautomers and conformers were generated to maximize the number of conformers. For all the complexes, bound ligands were used. Structures of these compounds were procured from DrugBank [51], and were subjected to the identical LigPrep procedure. After this, Ligand Docking process of the Glide program was initiated [52]. Precision was set to SP (Standard precision) and Ligand Sampling was set to Flexible. 10 poses were generated for each ligand and poses having the least binding energies amongst them were evaluated. 2D-interaction diagrams were visualized via Ligand Interactions. Additionally, molecular descriptors of these compounds were calculated via the QikProp module and assessed accordingly [53].

2.4. Microarray analyses of novel-indole benzimidazole derivatives and comparative transcriptomics

MCF-7 cells were exposed to compounds 48, 49, 50, 51, and 53 for 24 h at a dose of 20 μM . Total RNA was extracted from each sample where DMSO control and 51, each, had two biological replicates (RNeasy Mini Kit (QIAGEN)) before performing microarray experiments using HuGene 2.0 ST platform (Affymetrix). Data were normalized via Transcriptome Analysis Console Software (V3.0.0.466) using default Affymetrix analysis parameters and *rma* using affy package [54]. For differential expression analysis of 51 ($n = 2$) in comparison with DMSO ($n = 2$), the *limma* toolbox of R was used [55]. Volcano plot of statistical significance against fold change between control and 51 treated MCF-7 cells was generated in MATLAB. For multiple probes hitting the same gene, the probe with the lowest adjusted p-value was used.

GSEA was performed for each compound separately with default parameters to calculate the KEGG pathway enrichment using MSigDB [56]. Significantly enriched pathways were chosen (false discovery rate (FDR) q value < 0.25); and commonly enriched KEGG pathways were reported. LINCS database was used to identify compounds with the most and least similar expression profiles to significantly up- and down-regulated gene lists obtained from 51 (top 150 and bottom 150 ranked genes according to their $\log\text{FC}$ values) [57].

Limma analyses were performed between expression profiles of 48–49 and those of 50–51–53 compound series to identify the significantly differentially expressed genes at the adjusted p-value < 0.05 . Pathway enrichment was done on the significantly up- and down-regulated genes between groups via STRING database with Reactome Pathways option while Venn Diagrams of unique and variably affected pathways were also shown [58,59].

For comparative transcriptomics, GSE35428, GSE7765 and GSE62673 were retrieved and normalized with *rma* [60]. Differential expression analyses of normalized dataset were done using *limma* between groups as follows: for GSE35428: E2, tamoxifen (4OHT), ICI 182780, Lasofoxifene, Bazedoxifene or Raloxifene and EtOH (control) treatments; for GSE7765: Dioxin and DMSO (control) treatments; and for GSE62673: AA depletion (AA (-)) and control samples. For GSE7765, the results from hgu133A and hgu133B were merged. For multiple probes hitting the same gene, the probe with the lowest adjusted p-value was used. For GSE35428 and for GSE62673 best jetset probesets were selected for further analysis [61].

Venn diagrams were generated to represent the expression pattern (i.e., \log_2 fold changes) of the significantly altered genes ($N = 2177$, p-value < 0.05 between 51 & E2; $N = 111$, p-value < 0.05 between 51 & Dioxin; $N = 1480$, p-value < 0.05 between 51 & AA (-)). KEGG pathway enrichment analysis was performed using the STRING database; and Venn diagrams were generated based on the lists of significantly enriched pathways. Obtained diagrams were further utilized to form contingency tables where counts of shared and unique up-regulated or downregulated genes were used in performing Fisher's exact test in R.

Genes altered more than one-fold (FDR adj p-value < 0.05), in response to treatment with 51, were selected for the correlation analysis. The Pearson's correlation coefficient between each pair of treatments was used for the hierarchical clustering and heatmap was performed using ComplexHeatmap toolbox in R [62].

2.5. RT-QPCR assays for validation of treatment effects in MCF-7

Differential effects of candidate compounds on selected genes, known to be modulated by E2, dioxin, AA depletion, and/or to have roles in cell cycle, DNA damage/repair, drug metabolism were evaluated via RT-QPCR (LightCycler 480 II–Roche) in MCF-7 breast cancer cells exposed to 40 μM of each compound for 24 h. Following exposure, total mRNA was isolated and collected using the RNeasy Mini Kit

(QIAGEN) according to the manufacturer's instructions. Total RNA was then converted into cDNA using RevertAid First Strand cDNA Synthesis Kit (Thermo Scientific). Logarithmically transformed relative expression ($-\Delta\Delta Ct$) levels were calculated based on *TPT1* as the reference gene and DMSO treatment as the control group. The results were analyzed via either One-way ANOVA followed by Tukey's multiple comparisons to evaluate the compound-based effects or a Two-way ANOVA to assess dose-dependent effects (GraphPad Prism (v. 6.05)). ComplexHeatmap toolbox in R was utilized; and GSE35428 (E2), GSE7765 (dioxin), and GSE62673 (AA (-)) logFC data for the tested genes were annotated on top of the RT-QPCR data, for comparative representation. A list of primers was given in Table A. 1.

3. Results

3.1. Design and synthesis of indole-benzimidazole derivatives

The synthesis of compounds (Scheme 2) was initiated from 4-chloro-benzenesulfonyl chloride. 4-(ethylsulfonyl)-1-chlorobenzene (**1**) and 4-(ethylsulfonyl)-1-chloro-2-nitrobenzene (**2**) were synthesized according our previous publication [42]. To a solution of 4-(ethylsulfonyl)-1-chloro-2-nitrobenzene (**2**) (5 mmol) in ethanol (5 mL), amine derivative (15 mmol) was added and heated under reflux until the starting material was consumed (determined by TLC, 8–48 h). Upon cooling the mixture, water was added. The resultant yellow residue was crystallized from ethanol or purified by column chromatography (cc) by using a mixture of hexane and ethyl acetate in varying concentrations as eluent (Table 1) [43]. 5-methoxy-indole-3-carboxaldehyde was synthesized from 5-methoxy-indole, *N,N*-dimethylformamide, and phosphorus oxychloride [63].

Compounds **3–12** (3.5 mmol) in EtOH (75 mL) were reduced by hydrogenation using 40 psi of H_2 and 10% Pd/C (40 mg) until cessation of H_2 uptake to obtain the catalyst before filtering off on a bed of celite and washing with EtOH, and concentrating the filtrate in vacuo [44]. The crude amine was used without purification (**13–22**) (see for details Experimental Section). A mixture of the appropriate *o*-phenylenediamine (1 mmol), related indole derivative (1 mmol) and $Na_2S_2O_5$ (40%) (2 mL) in EtOH (4 mL), was refluxed until starting materials were

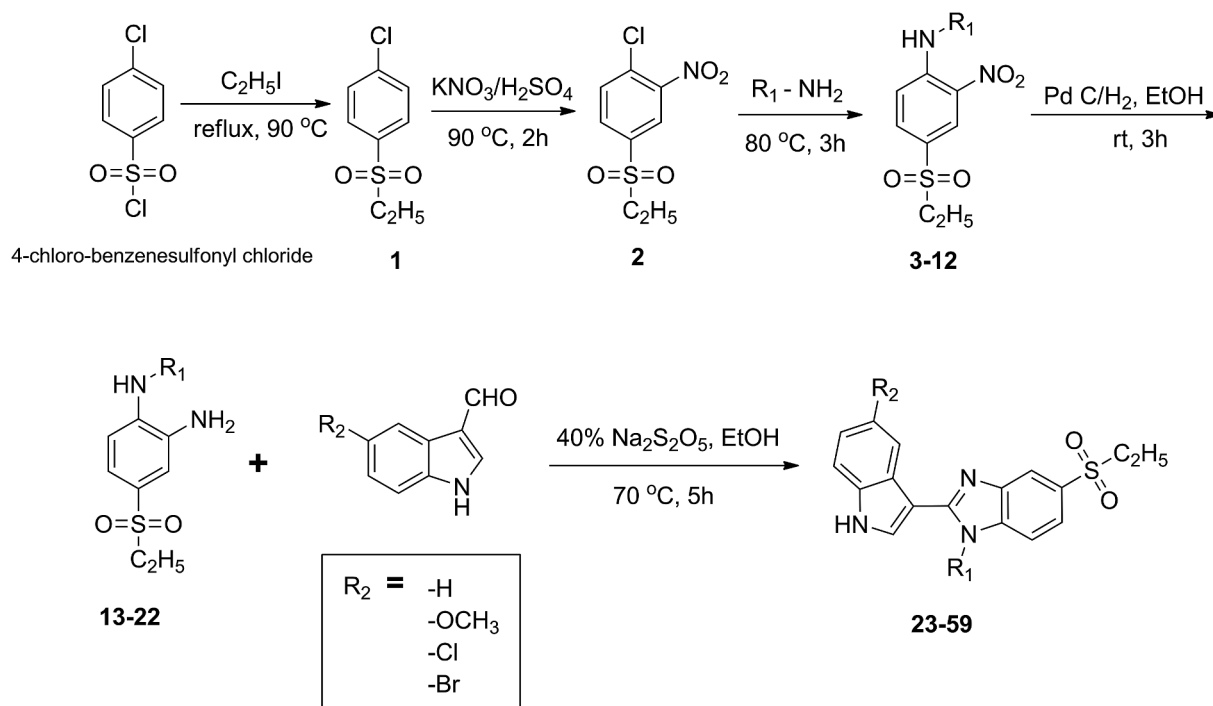
consumed (determined by TLC, 4–12 h). The precipitate was obtained upon pouring the reaction mixture and then filtering and washing. The residue was purified by cc to obtain the final product (**23–59**) [45]. The synthesis details of the compounds were provided in the Experimental Section.

3.2. Biological evaluation of indole-benzimidazole derivatives

3.2.1. Anti-cancer activity of novel indole-benzimidazole compounds in MCF-7 cell line

All ethylsulfonyl derivatives were analyzed for their cytotoxicity using MTT assays. A four-dose (0.25 μM , 2 μM , 16 μM and 40 μM) screening panel in MCF-7, an ER+ and TP53 (p53) wild-type breast cancer cell line, was used to identify highly effective compounds. This allowed us to screen large numbers of derivatives before pursuing selected compounds in more detail. As a result, the primary anticancer activity screening in MCF-7 showed that most of the compounds exhibited significance at one or more of the concentrations (Table 2). Hierarchical clustering of the compound relative cell viabilities (at log2 scale) helped summarize similarities between activities across doses (Fig. 2). Accordingly, molecules numbered **23**, **35**, **53**, **36**, **27**, **29**, **45**, **37**, **50** and **51** clustered together, since they were highly effective at the highest dose, and one or more of the other three concentrations. The remaining compounds were less effective than the above-mentioned compounds with respect to their level of activity. In addition, compound **49** was highly effective at the highest dose, i.e., 40 μM , yet was not effective at lower doses (Fig. 2). None of the molecules exhibited activity at the lowest dose (0.25 μM).

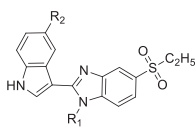
Synthesized compounds had either -H, -OCH₃, -Cl, or -Br at their R₂ position for each of the R₁ (Table 2). Therefore, the most active molecule could be determined for each of the R₁. According to the *n*-way ANOVA, molecular substitutions by R₁ and R₂ resulted in alterations on cytotoxic activities of the sulfonyl ethyl structures (p-value < 2e-16) where the R₁ group was the major predictor (p-value < 2e-16) of anticancer activity rather than the R₂ group (p-value: 0.0885). However, there was a significant interaction between R₁ and R₂ groups based on the cell viability scores (R_{1x2} interaction p-value < 2e-16) suggesting that substitution on indoles could modify the activity of



Scheme 2. Synthesis of new indole-benzimidazoles (23–59).

Table 2

Relative cell viability from four-dose screening with the ethylsulfonyl derivatives in MCF-7 cells. p-values were calculated using One-Way ANOVA followed by multiple comparisons.



No	R ₁	R ₂	% Relative viabilities				p-values			
			40 μM	16 μM	2 μM	0.25 μM	40 μM	16 μM	2 μM	0.25 μM
23	-H	-H	24.36	67.57	100	110.16	0.0000	0.0005	1.0000	0.2498
24	-H	-Br	67.53	85.44	90.04	105.73	0.0055	0.0391	0.2914	0.9979
25	-CH ₃	-H	64.68	72.12	94.01	95.39	0.0000	0.0293	0.9361	0.9238
26	-CH ₃	-OCH ₃	63.70	65.96	87.64	111.74	0.0028	0.0002	0.1572	0.9931
27	-CH ₃	-Cl	40.38	48.75	60.56	86.70	0.0001	0.0000	0.0000	0.1723
28	-CH ₃	-Br	69.58	79.32	94.45	92.97	0.0000	0.0089	0.0426	0.5252
29	-C ₂ H ₅	-H	44.16	45.09	77.02	87.82	0.0000	0.0000	0.0150	0.2749
30	-C ₂ H ₅	-OCH ₃	72.80	74.36	93.02	97.33	0.0112	0.0000	0.3659	0.9644
31	-C ₂ H ₅	-Cl	66.03	79.80	85.35	86.52	0.0000	0.0102	0.0001	0.1001
32	-C ₂ H ₅	-Br	58.80	58.13	85.41	111.86	0.0012	0.0000	0.0862	0.9742
33	-C ₃ H ₇	-H	69.52	98.64	101.48	112.94	0.0000	0.9871	0.9979	0.1720
34	-C ₃ H ₇	-OCH ₃	69.76	99.09	91.76	91.25	0.0000	0.9961	0.7629	0.4445
35	-C ₃ H ₇	-Cl	26.90	68.60	92	97.79	0.0000	0.0003	0.7776	0.9773
36	-C ₃ H ₇	-Br	32.85	48.06	77.12	89.86	0.0000	0.0000	0.0089	0.3313
37	-C ₄ H ₉	-H	43.76	55.21	91.36	101.55	0.0000	0.0000	0.3874	0.9919
38	-C ₄ H ₉	-Cl	89.88	81.38	94.29	110.80	0.0760	0.0021	0.6895	0.2854
39	-C ₄ H ₉	-Br	62.15	88.91	100.98	101.15	0.0009	0.4355	0.9990	0.9993
40	-cyclohexyl	-H	42.19	83.28	103.84	108.25	0.0005	0.8736	0.1878	0.9742
41	-cyclohexyl	-OCH ₃	64.12	85.42	91.05	102.61	0.0000	0.0008	0.3503	0.9805
42	-cyclohexyl	-Cl	63.80	82.62	97.92	105.45	0.0025	0.0498	0.9865	0.9742
43	-cyclohexyl	-Br	68.96	80.98	88.39	93.54	0.0000	0.0001	0.1768	0.7885
44	-benzyl	-H	89.26	95.42	104.85	99.40	0.0957	0.5882	0.3247	0.9979
45	-benzyl	-OCH ₃	39.58	54.85	84.41	95.28	0.0000	0.0000	0.0585	0.9010
46	-benzyl	-Cl	80.60	109.71	93.24	92.42	0.0700	0.3435	0.7116	0.9931
47	-benzyl	-Br	79.31	85.37	91.90	91.11	0.0456	0.0000	0.2589	0.4536
48	-p-fluoro benzyl	-H	59.55	92.02	92.69	93.24	0.0012	0.4955	0.6626	0.9979
49	-p-fluoro benzyl	-OCH ₃	52.00	92.06	105.67	105.33	0.0000	0.0124	0.1202	0.7249
50	-p-fluoro benzyl	-Cl	40.52	46.74	96.32	109.39	0.0000	0.0000	0.3942	0.3171
51	-p-fluoro benzyl	-Br	45.69	46.37	97.05	106.44	0.0000	0.0000	0.5654	0.6023
52	-3,4-difluorobenzyl	-H	73.53	92.77	85.60	101.92	0.0190	0.8907	0.3750	0.9918
53	-3,4-difluorobenzyl	-OCH ₃	33.53	43.94	86.09	95.01	0.0000	0.0000	0.0748	0.8098
54	-3,4-difluorobenzyl	-Cl	65.13	70.69	91.71	90.78	0.0000	0.0003	0.3661	0.4076
55	-3,4-difluorobenzyl	-Br	66.23	75.12	93.55	95.20	0.0000	0.0009	0.5591	0.8262
56	-3,4-dichlorobenzyl	-H	84.14	91.57	104.71	99.27	0.1014	0.6394	0.9074	0.9998
57	-3,4-dichlorobenzyl	-OCH ₃	86.39	90.78	90.94	106.51	0.0110	0.2980	0.3872	0.8039
58	-3,4-dichlorobenzyl	-Cl	73.06	72.70	100.18	115.78	0.0001	0.0022	1.0000	0.2061
59	-3,4-dichlorobenzyl	-Br	81.31	71.81	94.90	100.67	0.0016	0.0018	0.7792	0.9997

benzimidazoles differentially. Analysis by GRcalculator tool indicated that p-fluorobenzyl R₁ group was one of the most effective R₁ moiety outstanding from the rest of the substitutions (p-value: 0.023) and other cyclic aromatic side chain groups (p-value: 0.012) (Fig. 3; Fig. A.1). In addition to the p-fluorobenzyl, the substitutions of methyl (as in compound 27) and propyl on R₁ exhibited anti-proliferative trends.

3.2.2. Anti-cancer activity of selected compounds on different cell lines

Upon analysis of Table 2, we selected, for further screening, several compounds that were highly effective in reducing viability at the highest dose 40 μM (compounds: 23 (24.36%); 27 (40.38%); 29 (44.16%); 35 (26.90%); 36 (32.85%); and 37 (43.76%)); 40 (42.19%); 45 (39.58%); 48 (59.55%); 49 (52.00%); 50 (40.52%); 51 (45.69%); 53 (33.53%) and a control molecule with relatively less cytotoxic activity (compound 46 (80.60%)). Among these, 48–51 spanning the full -p-fluorobenzyl series exhibited similar activity at 40 μM whereas 50 and 51 were also significantly antiproliferative at a relatively lower concentration of 16 μM along with another related compound 53 containing 3,4-difluorobenzyl group. In the wider dose panel, IC₅₀ values of these 13 molecules across multiple cell lines (Table 3) were studied along with *n*-way ANOVA. Overall, R₁ chain (p-value < 2e–16) had

significant effects on viability while the effect of the R₂ side chain was also significant (p-value < 2e–16) and varied depending on the type of R₁ (R₁×2 interaction p-value < 2e–16). Moreover, there was also a significant cell line effect (p-value: 2.62e–08) as well as a treatment effect (p-value < 2e–16). Additional analyses with two-way ANOVA and multiple comparison tests have implied possible trends by cell line and R₂ (Table 3; Fig. 4; Fig. A.3; Fig. A.4). Cell line specific effects in response to treatments were observable via Principal Component Analysis (PCA) where both MCF-7 and HEPG2 lines interestingly yielded parallel profiles in comparison to MDA-MB-231 (Fig. 4). PCA showed that E2 responsive cell lines MCF-7 and HEPG2 were more similar to each other than they were to the ER- MDA-MB-231 cells at lower concentrations (up to 16 μM) while at the highest dose tested (40 μM) each cell line assumed a relatively distinct response profile. In particular, the compound 53 exhibited low IC₅₀ values for the TP53 wild-type MCF-7 and HEPG2 cells (19.23 μM and 24.10 μM, respectively) while it was not as effective in MDA-MB-231, a cell line with a mutant TP53 allele. In accord with two-way ANOVA comparisons, most of the candidate compounds exhibited a cell-line dependency, but not compound 37 with butyl (R₁) and -H (R₂) substitutions (Table 3; Fig. A.4). Nonetheless, GRcalculator assessments showed that MCF-7 was the cell

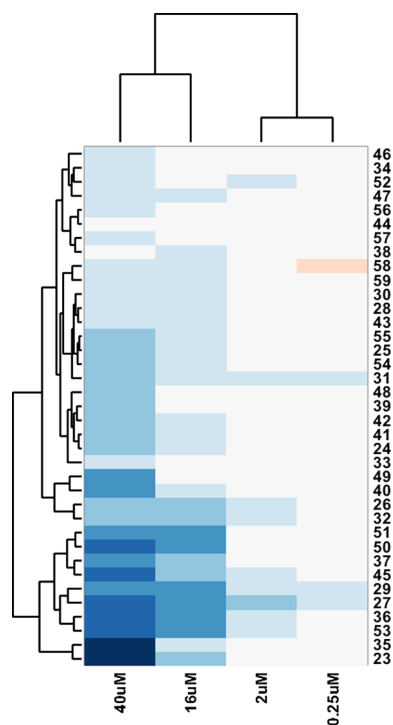


Fig. 2. Hierarchical clustering of anti-cancer activity of the novel indole-benzimidazoles. Darker tones of blue indicate stronger inhibition of cell growth. Euclidean distance and complete linkage were used for clustering (MATLAB®).

line that seemed to be affected the most by the compounds, whereas -Br carrying R_2 moieties on the Table 2 compounds were also observed to have more effect on viability (Fig. A.2; Fig. A.3). After obtaining the toxicity data, we continued with docking studies and transcriptomic

analyses in order to get an understanding on the mechanisms of action.

3.3. Molecular docking studies

Structurally related R_1 groups with relatively high potencies were taken into docking analyses. On the basis of the literature on indoles and benzimidazoles as well as PCA clusters in this study, we primarily focused on ER α , and assessed dockings of R_1 :p-fluorobenzyl derivatives and **53**. Compound based statistical comparisons between the cell lines were also in accord with these observations (Fig. A.2). Our indole-benzimidazole derivatives tended to exhibit increased affinity to ER α , VEGFR2, and tubulin rather than the other ones which were discussed in Section 2.3, such as Protein kinase C beta II, glycogen synthase kinase 3, Platelet-derived growth factor receptor beta.

Based on the structural analysis (Fig. 5) ER α ligand binding domain mainly consists of hydrophobic residues. Therefore, utilization of hydrophobic moieties such as indole and benzimidazole may play a key role in inhibiting or activating this receptor. The binding mode of 4-hydroxytamoxifen with ER α suggested that a hydrogen donor group could be important for H-bond interaction with polar residue Gly521 in this cavity. This interaction's distance was 2.28 Å. In the literature, these residues including Glu353, Arg394, Phe404 and Lys529 take part in the modulation of this receptor. Hydrophobic interactions with Phe404 and Trp383, H-bond interactions with Glu353 and Arg394, also a salt bridge interaction with Asp351 are important according to both bazedoxifene and 4-hydroxytamoxifen's patterns [64]. List of molecular properties and ER α docking energies for all compounds were given in Table A. 10.

One of the prominent compounds that stood out in transcriptomic analyses, compound **51**, created halogen bond interactions with both Glu353 and Arg394. In the case of the another potent ligand **53**, Phe404 joins a Pi-Pi interaction with an indole ring while the sulfonyl group acts as the hydrogen bond donor (Fig. 6). Both ligands have provided necessary interactions in the reference study. Their energy values were relatively close to that of standard compound bazedoxifene.

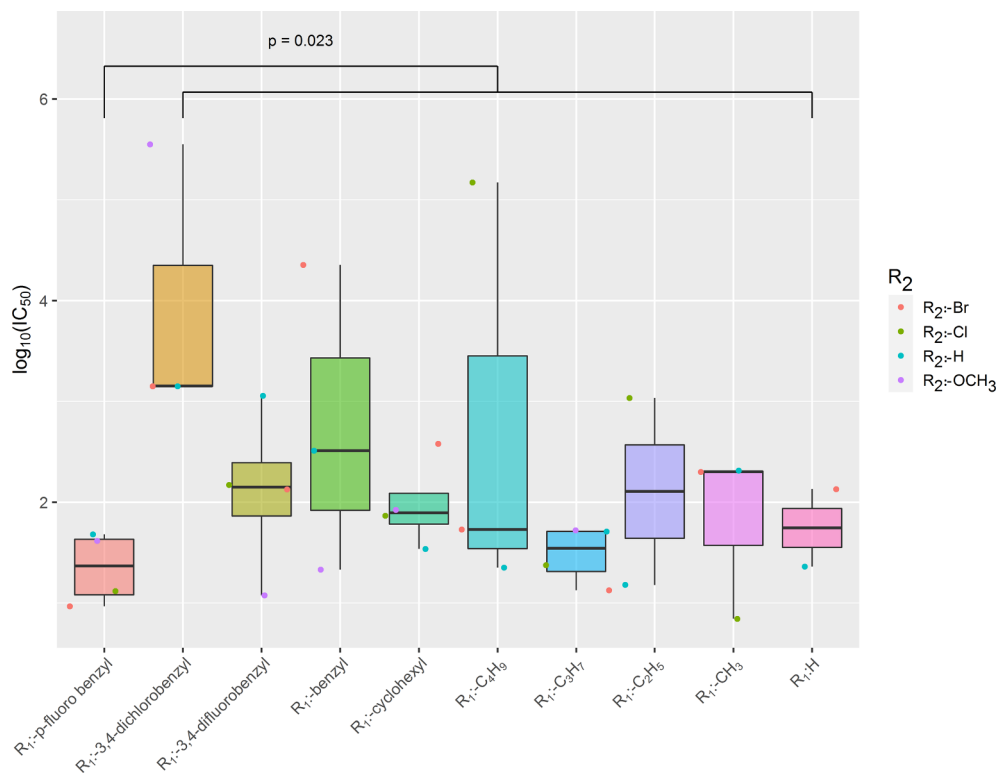


Fig. 3. Log₁₀(IC₅₀) based representation and comparison of R_1 carrying derivatives (GRcalculator tool was used for this purpose and comparisons between all derivatives versus p-fluorobenzyl substituted compounds were made with a built-in one-sided Wilcoxon rank-sum test).

Table 3

IC₅₀ (μM) values and two-way ANOVA cell line specific p-value for each selected candidate tested on MCF-7, MDA-MB-231 and HEPG2 cells (NA: Unmeasurable IC₅₀ values, ns: not significant).

Comp.	IC ₅₀			Cell line effect p-value	Comp.	IC ₅₀			Cell line effect p-value
	MCF-7	MDA-MB-231	HEPG2			MCF-7	MDA-MB-231	HEPG2	
23	42.9536	51.4043	47.9733	< 0.0001	45	32.2849	22.3872	9.9540	< 0.0001
27	5.71	NA	NA	< 0.0001	46	43.4510	10.9396	89.54	< 0.0001
29	89.3305	NA	73.7904	< 0.0001	48	27.2270	20.8450	78.70	< 0.0001
35	54.4503	126.7652	32.7341	< 0.0001	49	39.5367	44.2588	41.11	< 0.0001
36	15.7398	49.8884	7.8163	< 0.0001	50	18.0717	36.1410	58.6138	< 0.0001
37	30.4089	66.6807	31.5500	0.3538 (ns)	51	35.1560	38.2825	17.2584	< 0.0001
40	40.2717	76.9130	NA	< 0.0001	53	19.2309	NA	24.0991	< 0.0001

According to the glide docking score results in Table 4, compounds 48, 49 and 51 have exhibited favorable affinity value against ER when compared with those against tubulin and vEGFR2.

3.4. Gene level alterations upon exposure to indole-benzimidazoles

3.4.1. Transcriptomics analysis of compounds 48–51 and 53

Based on Fig. 3, derivatives with p-fluorobenzyl and the structurally related compound 53 represented strong candidates for understanding the molecular mechanisms of action of the effective novel indole-benzimidazoles. For that purpose, we initiated gene level analyses in a parallel line with molecular docking studies. *Limma* analysis of expression data obtained upon exposure to compound 51 demonstrated that MCF-7 transcriptome was significantly modulated leading to up-regulation and downregulation of a considerable number of genes (Fig. 7; Table 5).

Additionally, the STRING protein-protein interaction network and KEGG pathway analyses for the compound 51 were implemented to reveal various molecular pathways that might be involved in the anticancer effects of the derivatives (Table A. 2). Accordingly, stress mechanisms, apoptosis and ferroptosis, as well as p53 and cellular signaling via MAPK pathway, were observed in addition to the metabolic process of aminoacyl-tRNA biosynthesis. List of these pathways were also common when the gene signatures of the compounds 50, 51 and 53 are compared, confirming similarity of the derivative exposures on molecular level (Table A. 3). In addition to that, overall comparisons with all the microarrayed compounds together resulted in a relatively limited set of mutual pathways such as cell cycle and DNA replication (Table A. 4) which might be due to milder effects on the expression by

the compounds 48 and 49 at 20 μM. Candidate pathways as well as dose-dependent effects were further taken into account in understanding the mechanisms of action of these derivatives. We compared the expression profiles of compounds 48–49 with those of 50–51–53 showing that 553 genes were differentially expressed between these two groups (adjusted p-value < 0.05). Pathway enrichment by STRING – Reactome Pathways demonstrated that compounds 50–51–53 led to significantly more reduction in expression of genes related with cell cycle and ESR1 signaling while increasing the stress response in MCF-7 cells (Fig. A.5; Table A. 5).

3.4.2. LINC analysis

Query of the top 150 up- and 150 down-regulated genes by 51 against a large collection of compounds, gene knockdown and gene overexpression datasets obtained from MCF-7 cells was performed using LINC database and the most positively and negatively correlated compounds were provided (Table 6; Table A. 6). Among the compounds most similar to 51 were the inhibitors of various classes such as ER antagonists, calcium channel inhibitors (niguldipine, an amino acid (AA) response/integrated stress response activator [65]), tubulin and microtubule inhibitors. Besides, three out of the top ten compounds also were carrying indole or benzimidazole backbones. Interestingly, the top compound oxindole-I and an ER antagonist, i.e., ZK-164015, were among them. Many of the tubulin and microtubule inhibitors from this analysis were also found to carry either an indole or benzimidazole scaffold (Table A. 6).

3.4.3. Comparative transcriptomics

Comparative transcriptomics analysis of the selected indole-

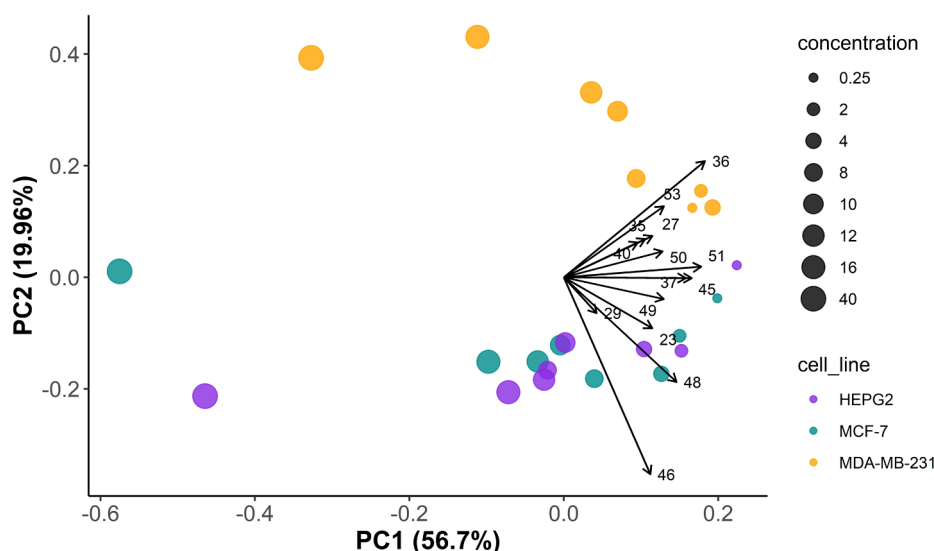


Fig. 4. PCA representation on cell viabilities of the cell lines upon exposure to varying concentrations of novel derivatives.

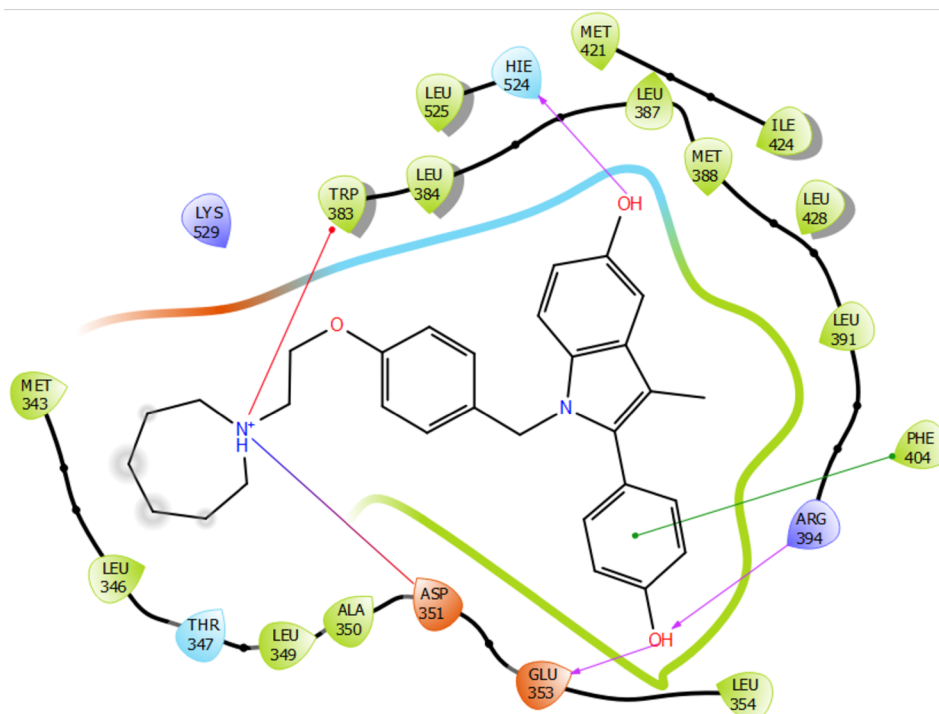


Fig. 5. 2D diagram of amino acid interactions of bazedoxifene with ER α ligand-binding domain. Hydrophobic interactions are shown as green, whereas the red line represents Pi-cation interactions. H-bond interactions are depicted as purple. Red-blue represents salt bridge interaction.

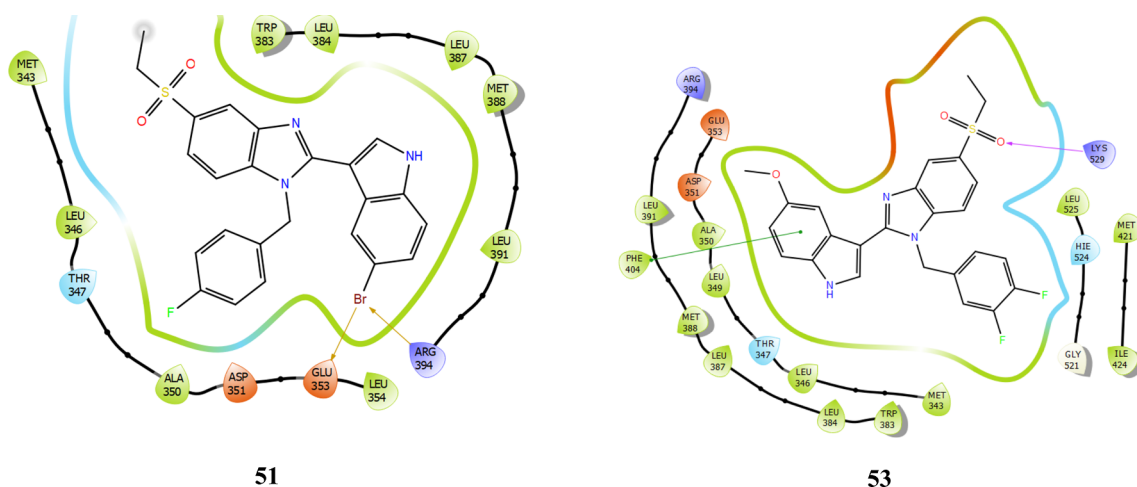


Fig. 6. 2D interaction diagrams of the two most potent compounds against MCF-7 and in microarray analyses. Brown arrow indicates halogen bond interaction and purple one indicate hydrogen bond interaction, whilst green line represents Pi-Pi steric interaction.

Table 4

Data showing the glide scores of microarrayed compounds against different proteins.

Compounds	ER α	Tubulin	vEGFR2 kinase domain
48	-7.776	-5.851	-6.348
49	-7.726	-5.575	-6.786
50	Unsuccessful binding	Unsuccessful binding	-6.435
51	-7.802	-5.458	-6.131
53	-6.610	-5.662	-6.813
Vincristine	-	-8.1	-
Tivozanib	-	-	-10.265
Bazedoxifene	-9.852	-	-

benzimidazoles was performed using public microarray datasets for AA (-) and exposure to E2/SERMs or dioxin, an aryl hydrocarbon activator known to be activated by plant-based estrogens [66–68]. This approach has further demonstrated a pattern of inverse correlation with E2 and positive correlations with SERMs, AhR/dioxin, and AA (-) signatures (Fig. 8). AA deprivation was the most closely associated treatment followed by dioxin and SERMs while indole-benzimidazoles formed the tightest cluster. Our results showed that novel indole-benzimidazoles exhibited transcript-level effects that were more pronounced than the generic SERMs on reverting E2 driven expression modulation. Furthermore, compounds 50, 51 and 53 were found in the same cluster while compounds 48 and 49 formed another cluster which was placed closer to the generic SERMs. In accord with this expression profile based clustering, compounds 48 (R₂: -H) and 49 (R₂: -OCH₃) had higher IC₅₀ values, thus lower drug effectivity than 50 (R₂: -Cl), 51 (R₂: -Br) and 53 (R₁: 3,4-difluorobenzyl; R₂: -OCH₃) (Fig. A.4).

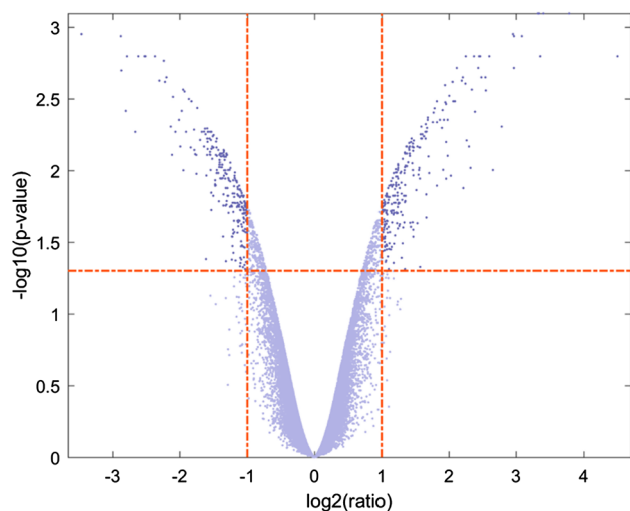


Fig. 7. Volcano plot of statistical significance against fold change between control and compound **51** treated MCF-7 cells. 546 genes were statistically altered more than two folds (adjusted p-value with FDR < 0.05).

To further investigate how expression profiles of novel indole-benzimidazole compounds relate with those obtained from E2 exposure, AA depletion and dioxin treatments, we performed KEGG pathway [69] enrichment analyses using GSEA [70,71]. The numbers of significantly affected genes between exposures to E2 and compound **51** were represented using a Venn diagram and enriched pathways were indicated (Fig. 9; p-value < 0.05 (compound **51** & E2)). According to the comparisons with E2 exposure in MCF-7 cells, the inversely associated signaling pathways included upregulation of TGF- β pathway and downregulation of DNA replication, cell-cycle, mismatch repair, pyrimidine metabolism, cysteine and methionine metabolism and spliceosome pathways by the novel indole-benzimidazole compounds. Mutually upregulated and downregulated pathways were provided in Table A. 7. Interestingly, the downregulation of similar pathways, but this time in the same direction, were observed in the comparisons performed with **51** versus AA (-), whereas dioxin versus **51** revealed involvement of steroid and amino acid related metabolisms, including downregulation of E2 signaling pathway. Furthermore, the term “ferroptosis” was enriched in mutually upregulated pathways for both dioxin and AA (-) and **51** profile. Fisher’s exact tests showed significance (Table A. 7).

3.4.4. Validation of molecular pathways by RT-QPCR in MCF-7 cells

High throughput comparative transcriptomic analysis led to the identification of several pathways and genes whose expressions were altered upon exposure to the novel derivatives as well as E2, one or more SERMs, dioxin or AA depletion. For validation by RT-QPCR, we

Table 5

The top 10 significantly altered genes in compound **51** treated samples. Adjusted (Adj.) p reflects the FDR corrected p-value, calculated with *limma*.

Downregulated				Upregulated			
Gene Symbol	LogFC	p-value	Adj.p value	Gene Symbol	LogFC	p-value	Adj.p value
FAM111B	-3.46	1.38E-07	0.001	SLC7A11	4.5	5.09E-07	0.002
IGFBP5	-2.87	1.21E-06	0.002	FAM129A	3.78	2.84E-08	0.001
GRPR	-2.8	4.62E-06	0.004	ERRF1	3.4	6.66E-08	0.001
TARP	-2.79	7.62E-07	0.002	MT1F	3.35	5.07E-07	0.002
GINS2	-2.62	7.15E-07	0.002	CLGN	3.35	4.34E-07	0.002
CCNE2	-2.52	4.74E-07	0.002	GDF15	3.33	6.56E-08	0.001
DTL	-2.51	5.47E-07	0.002	CYP1A1	3.31	5.57E-08	0.001
MCM10	-2.37	6.26E-07	0.002	SLFN5	2.97	1.83E-07	0.001
UCA1	-2.3	1.71E-06	0.002	DDIT3	2.97	1.11E-06	0.002
IL20	-2.23	8.91E-07	0.002	ANXA3	2.96	1.39E-07	0.001

Table 6

Top 10 ranking compounds that possess transcriptomic similarity with **51** in MCF-7 line. Compounds with either indole or benzimidazole moieties are given with bold characters.

Rank	Score	Name	Description
1	99.98	oxindole-1	VEGFR inhibitor
2	99.98	niguldipine	Calcium channel blocker
3	99.97	AG-592	Tyrosine kinase inhibitor
4	99.96	AG-879	Angiogenesis inhibitor
5	99.96	FCCP	Mitochondrial oxidative phosphorylation uncoupler
6	99.96	ZK-164015	ER antagonist
7	99.96	reserpine	Vesicular monoamine transporter inhibitor
8	99.96	PD-198306	MAP kinase inhibitor
9	99.96	CGK-733	ATR kinase inhibitor
10	99.96	suloctidil	Adrenergic receptor antagonist

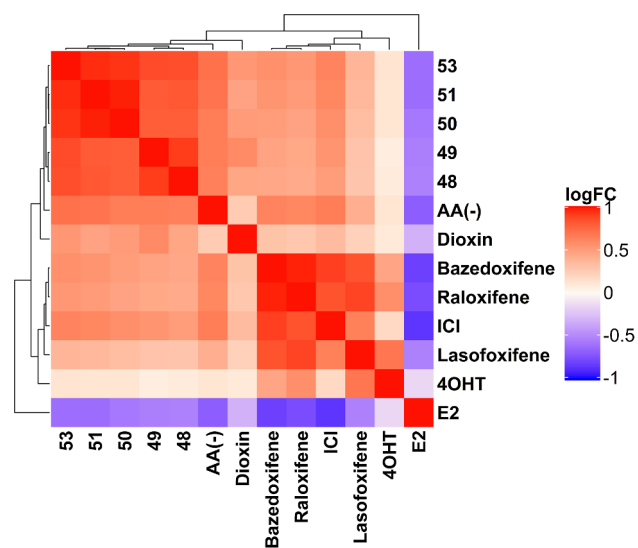


Fig. 8. Clustergram analysis of the pairwise-correlation between generic SERMs and compounds **48**, **49**, **50**, **51** and **53**. The genes were selected with the p-value (< 0.05) and log fold difference (> 1) cut-offs for compound **51**. Ward linkage and Euclidian distance were used for the clustering. Red indicates positive correlation while blue indicates negative correlation in between samples on the heatmap.

identified multiple genes that were modulated by E2, dioxin or AA deprivation and/or involved in cell cycle, integrated stress response, and drug metabolism (Fig. 10).

Our findings first showed that minor structural differences could contribute to detectable changes on the expression of the genes we analyzed (Fig. 10; Table A. 8; Table A. 9). For example, the compounds **49**, **50** and **51** have influenced *CDKN1A* expression remarkably, while

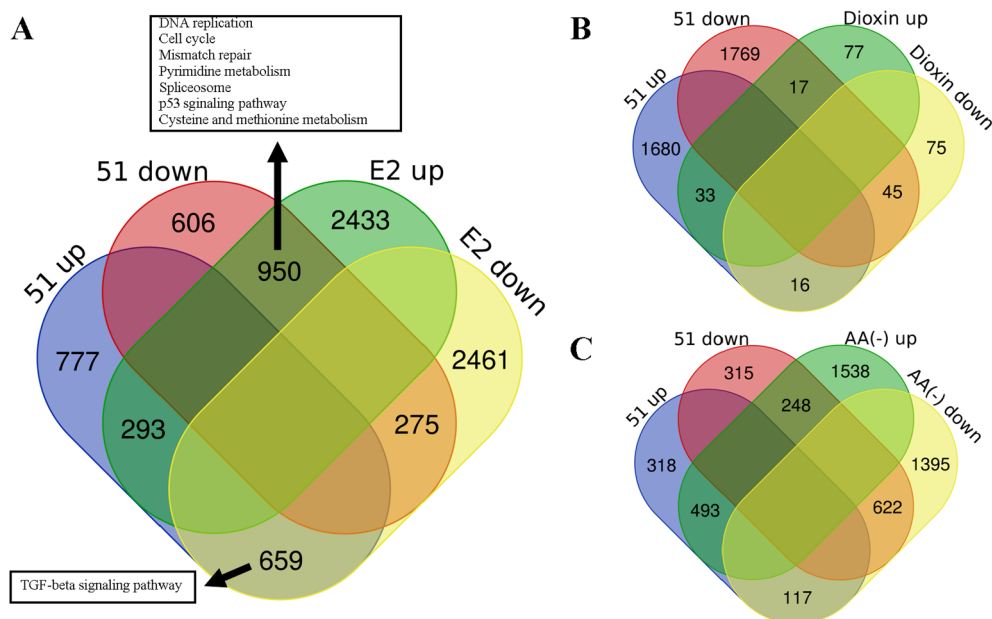


Fig. 9. KEGG pathway enrichment analysis results for Compound 51 and (A) E2, (B) Dioxin and (C) AA (-). Significantly enriched (p -value < 0.05) genes and related pathways that are mutually affected are depicted, especially for E2 comparisons. Fisher's exact p -values are (A) < $2.2e-16$, (B) $4.415e-05$ and (C) < $2.2e-16$. Detailed list of enriched pathways (for A, B and C) and the contingency table for the comparisons are provided in Table A. 7.

the compound **48** (R_1 : -H) was less effective. Moreover, compounds **51** and **53** caused significant decreases in *ANLN* expression and **48** and **50** were additionally more effective in altering the levels of *WDHD1*. Interestingly, *GADD45A* expression was modulated by compounds **48**, **50** and **51** while compound **49** did not lead to overexpression of *GADD45A*. Compound **53** containing 3,4-difluorobenzyl at R_1 position also induced *CDKN1A* and *GADD45A* expression while having reduced expression of cell cycle related genes (at both *ANLN* and *WDHD1*). Further taking GSE35428 and GSE7765 data into account, the exposures to E2 and indole-benzimidazole were found to be inversely associated implicating the derivatives investigated herein as E2 antagonists. In addition to the E2 signaling, *CYP1B1* and *HMOX1* were also upregulated by AhR agonist dioxin while changes in *DDIT3*,

SLC7A11 and *HMOX1* were similarly affected by indole-benzimidazoles and AA depletion which further suggested the involvement of multiple mechanisms in compound responses. Later analyses, where we compared gene expression levels of the primary E2 target genes, *CCND1*, *TFF1* and *PGR*, using different exposure concentrations (20 μ M vs 40 μ M), also presented additional confirmation on the dose-dependent relationship between the derivatives and E2 signaling (Fig. A.6). Here, only *TFF1* gene represented a dose-dependent difference (p -value: 0.0207) whereas *CCND1* and *PGR* did not (p -values: 0.6284 and 0.4252, respectively). Moreover, the microarray and RT-QPCR experiments performed with doses of 20 μ M and 40 μ M respectively, had shown that compounds **50**, **51** and **53** yielded stronger effects on the expression of these genes. However, a 40 μ M exposure to **48** or **49**

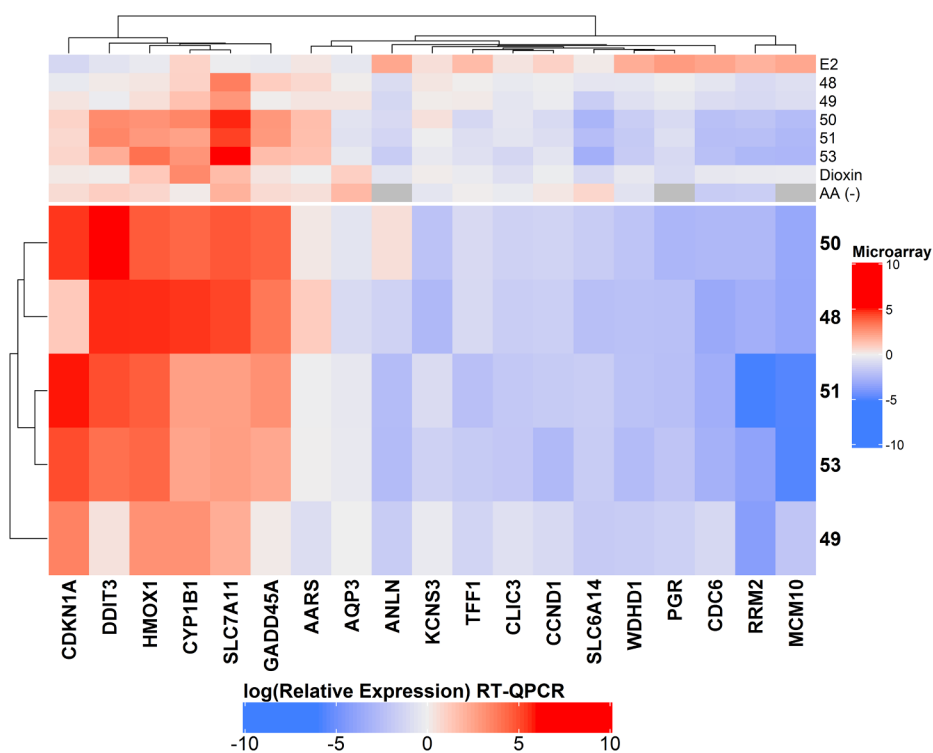


Fig. 10. Validation of selected AhR/dioxin, integrated stress response/AA (-), and E2/SERM modulated genes by RT-QPCR in MCF-7 cells exposed to the compounds **48**, **49**, **50**, **51** and **53** for 24 h at 40 μ M. Relative quantity (RQ) values are depicted in log₂ and color scale (blue-to-red (negative-to-positive)). *TPT1* is used as the house-keeping gene; along the x-axes, the compound names were given. Top annotation values are gathered from three different public datasets and our own microarray data; and log fold change values are represented for the corresponding genes in a color scale (blue-to-red (negative-to-positive)) where gray points represent missing values due to microarray platform used in aminoacid depletion study. Exact log₂ relative quantity values and significance signs can be accessed in Table A. 8 and Table A. 9. (For interpretation of the references to colour in this figure legend, the reader is referred to the web version of this article.)

exhibited similar responses when compared with the other three molecules investigated, suggesting a dose-dependent increase in transcriptional response.

4. Discussion

In the present study, we have synthesized and characterized a set of novel indole-benzimidazoles carrying benzene sulphonyl structures, to assess their cytotoxicity, structural affinity to potential targets (mainly ER), molecular expression profiles and association with the regulators of anticancer pathways. Accordingly, we found most of our compounds significantly reduced the cell viability of ER+ MCF-7 cells, especially at a concentration equaling to 40 μ M. In addition, we have utilized different statistical tools to understand the structure-activity relationships (SARs) better. For that purpose, we have analyzed our data using ANOVA and multivariate techniques such as PCA and hierarchical clustering which proved valuable to make distinctions among the compounds with respect to dose, molecular group, and cell line differences. Regarding the substitutions (Table 1 & Table 2), both R₁ and R₂ groups were found to be important in altering the anticancer effect of the indole-benzimidazole scaffold. However, there was a significant interaction between these two groups of which future studies should take into consideration.

Structurally related R₁ group members (48, 49, 50 and 51) exhibited single position changes yet showed differential anti-proliferative activity on MCF-7 cells. In addition, this group had the lowest average IC₅₀ values when compared with the other molecule series warranting further analyses. Our strategy also involved differential expression profiling of MCF-7 cells exposed to compound 51 exhibiting the lowest growth inhibition at 16 μ M, along with compound 50, followed by stringent transcriptomics comparisons across full series and with an additional related compound 53 from R₁:3,4-difluorobenzyl group, exhibiting even stronger anti-proliferative effects towards E2 responsive cell lines. Future studies should consider extending the above mentioned approach to other compound series and cell lines with differing characteristics to better understand the molecular mechanisms by which novel indole-benzimidazoles exert their effects.

The differences observed in cell viability profiles can be due to multiple factors, such as the dose and/or tissue specificity (breast vs. liver) as well as the cell line's batch, molecular receptor status (e.g., ER and AhR) and pathway activity (e.g., TP53 and AA (-) stress). For example, compound 53, whose microarray-based molecular effects (20 μ M) closely resembling those of compounds 50 and 51 in MCF-7 cells, might lead to a different expression profile in the ER-/TP53 mutant MDA-MB-231 cell line, exhibiting lower sensitivity to 53. On the other hand, a compound which is similarly active in the breast cancer cells based on IC₅₀ values can be more active in another batch or type of cancer cell line, as in the case of compound 51. In conclusion, although our structural models have suggested potential affinity to ER for compounds 51 and 53, a comparative transcriptomics approach further demonstrated that downstream molecular effects of these novel indole-benzimidazoles are likely to be driven via multiple routes/pathways (e.g., AhR), and not just ER. This notion can further explain the observed cell- and dose-dependent differences in anti-cancer activity.

Taking the docking results into account, one possible reason of the higher activity shown by compounds 51 and 53's could be the increased amount of halogen bond (a type of H-bond) interactions. Also, the presence of bromine group may enhance lipophilic characteristic of indole moiety creating a more successful binding pattern. Therefore compound 51 was elected as a possible candidate for future assessment and pharmacokinetic development studies. Unsuccessful ER binding profile obtained for the compound 50 was an unexpected case, considering its similarity to the compounds 51 and 53 based on the gene expression and cytotoxicity results obtained. Although the situation here is suggestive for alternative binding profiles towards ER or other protein targets, such cases demand further re-evaluations, primarily *in*

silico. In addition, glide scores overall yielded positive results, even though observed affinity levels were lesser in the derivatives than the standard compounds, meaning that the derivatives had the tendency to form stable ligand-protein complexes with ER α . Moreover, it was clear that ER α might not be the only binding target of the derivatives, but also some other proteins in inducing cell death. Nevertheless, in this current study, *in silico* findings and literature investigations [72,73] nominate ER α as the most favorable indole-benzimidazole target in comparison to ER β , tubulin and vEGFR.

Aside from docking studies, the expression profiling of compounds 48–51 (R₁:p-fluorobenzyl; R₂:-H, -OCH₃, -Br, -Cl) and 53 (R₁:3,4-difluorobenzyl; R₂:-OCH₃) and comparative transcriptomics with public datasets have significantly increased our understanding of the molecular mechanisms mediating the effects of indole-benzimidazoles in ER + breast cancer cells. The use of comparative transcriptomics and RT-QPCR analyses further validated and supported our findings. Previously, altered expression of cell cycle, DNA replication, endoplasmic reticulum stress and DNA damage response-related processes have been reported in MCF-7 cells when exposed to CTet, an indole-3-carbinol derivative [74,75]. However, herein we, for the first time, show significant and positive associations between the expression profiles of indole-benzimidazoles and those of the selected ER antagonists, AhR agonist dioxin, and AA deprivation. Furthermore, these comparative transcriptomics approaches implicate indole-benzimidazoles in simultaneous modulation of multiple cancer-relevant pathways leading to a strong anticancer behavior in a dose-dependent manner, where the effects were more profound for 50, 51 and 53 at 20 μ M, than the compounds 48 and 49.

STRING analyses have shown that stress mechanisms, aminoacyl-tRNA metabolism and ferroptosis might be involved in these anti-cancer effects. For instance, aminoacyl-tRNA metabolism can be driven by steroids and sex hormones in breast cancer where the ER status of the cancer matters in cell proliferation rate, in return [76–78]. In addition, AA deprivation can affect the charging status of specific tRNA iso-acceptor, underlying interaction between abundant amino acids in the environment which further influences the efficiency of the translation processes [79,80]. The transcriptomic similarity between our derivatives and AA deprivation profiles further supports the involvement of aminoacyl-tRNA biosynthesis pathway where ER modulation can influence this pathway. Interestingly, aminoacyl-tRNA metabolism and AA signaling have regulatory roles also in ferroptosis which can further explain the selected derivatives' anti-cancer responses [81–83].

GSEA results also helped identify the conserved and associated alterations in the molecular/cellular pathways driven by 51 and E2, dioxin or AA (-) exposures. Results pointed to some shared mechanisms among the treatments that have been previously indicated with cancers. Among the associated pathways, TGF- β and cell cycle pathways have been widely studied while pyrimidine metabolism is one of the pathways more recently gained attention in breast cancer therapy [84,85]. Inversely correlated signatures between E2 and AA(-) further underlined the close relationship between amino acid metabolism and ER signaling [86]. Besides that, downregulation of ER signaling was a mutual mechanism between 51 and dioxin exposures further underlying ER modulatory roles for the indole-benzimidazoles and AhR signaling [66,68]. Moreover, aminoacyl and AA-related pathways, as well as ferroptosis, were among the enriched terms across multiple dataset comparisons strongly pinpointing crucial roles in the downstream effects of indole-benzimidazole derivatives.

Additionally, transcriptomic signature of the compound 51 had remarkable similarities with certain LINCS database compounds that were screened in MCF-7 cells. At the top of the most similar compounds was a multitargeting compound oxindole-I, which also carries an indole moiety and constitutes the pharmacophore of the drug sunitinib [87]. Derivatives of this compound have been found to be involved in generation of oxidative stress leading to cell death [88]. In support of that, double-stranded RNA-dependent protein kinase (PKR) that mediates

stress responses can be targeted by an imidazole-oxindole type derivative (C16 compound) also mediating ferroptosis in the end [89]. Additionally, its derivative compound sunitinib shares similar features on cell death with sorafenib, another known ferroptotic agent [90,91]. The presence of oxindole structure can also affect the aryl hydrocarbon receptor which is in a strong relationship with stress pathways, ferroptosis, amino acid metabolism and ER signaling [92–96]. Transcriptomic similarity with dioxin further supports the involvement of this pathway and others in downstream effects of indole-benzimidazole exposure. The second top hit compound, niguldipine, is a calcium channel blocker that can lead to unfolded amino acid stress response and ferroptosis [65,97]. One of the other top hit compounds were FCCP, a mitochondrial oxidative phosphorylation uncoupler and again a ferroptosis inhibitor [98], and ZK-164015, an ER antagonist containing an indole moiety. Moreover, the transcriptional profile of reserpine, another indole carrying structure, which also strongly influences the Nrf2-mediated anti-oxidative stress pathway [99] also has exhibited significant similarity with compound 51. The presence of indole or benzimidazole backbones in multiple ER modulators and tubulin inhibitors strongly supported the notion for the involvement of tubulin related mechanisms in response to indole-benzimidazole derivatives [100–102]. Even though *in silico* docking results revealed low potency of the derivatives in tubulin binding, actual binding and affinity profiles should be further tested via *in situ* experiments.

In this study we have identified several effective novel indole-benzimidazole compound series and found out that some bearing p-fluorobenzyl and alkyl groups on R₁ were active at concentrations lower than 40 μM. In addition, molecular profiling of five related compounds with varying anti-proliferative efficacies enabled us to address the association between levels of anti-proliferation and gene expression modulation. Molecular pathways contributing to drug efficacy included unfolded protein/stress response, cytosolic tRNA aminoacylation, ESR1 signaling and cell cycle. Accordingly the chemical structure of the relatively more active compounds 50, 51 and 53 could be used as templates for future designs.

Among the screened compounds, substitutions on R₂ were restricted to four bases only, and the alterations on R₂ moieties were able to affect the potency of R₁ bearing scaffolds differentially, suggesting that a wider scale of R₂ based substitutions holds potential for improvements in the activity levels. In addition to that, sulfonyl side chain groups were limited with ethyl substitutions only. Therefore, applications of other alkyl moieties as well as aryl groups demand further experiments [103]. In addition, *N*-benzylation of the derivatives could also enhance their activity levels [39].

Moreover, indole aryl sulfonamides are also known to act as aromatase inhibitors in ER+ MCF-7 cell line [103]. Accordingly, our novel compounds carrying these functional groups can exhibit similar activity with steroid based aromatase modulators warranting further study.

5. Conclusions

In conclusion, cellular, structural as well as comparative transcriptomic approaches have enabled us to gather valuable insights into the pharmacological action of the novel derivatives generated in this study. Analyzing the lead compounds in detail we have identified their antiestrogenic effects as well as novel mechanisms involving aminoacyl-tRNA metabolism, AA depletion mediated integrated stress response, ferroptosis and AhR pathway, all of which have not previously been assigned for indole-benzimidazoles. Our study has brought about the possibility that the derivatives can also have the ability to target multiple genes/pathways. Elucidation of the targets requires further study including advanced modeling approaches and functional interventions at the molecular level.

Some important SARs emerging from the present study could also be summarized as follows: indole-benzimidazoles that have either p-

fluorobenzyl or small alkyl groups at their R₁ position in addition to electron-withdrawing groups in R₂ might have relatively more effective anticancer activities. The compound 51 containing p-fluorobenzyl at R₁ position and -Br at R₂ position was one of the prominent compounds against MCF-7 cells as validated by microarray analyses as well as docking studies. Although the limited range of sample size and interaction between side-chain moieties obscure more definitive conclusions, applied statistical approaches underline the nature of R₁ and R₂ groups and their effects on multiple cell lines. Therefore, not only p-fluorobenzyl, but also difluorobenzyl (53), methyl (27) and propyl substitutions (36) on R₁ might warrant future studies where genotypes of the samples and applicable doses should be taken into account.

Binding profiles of the derivatives also supported the notion that there can be multiple targets involved in their cytotoxic action. As we have seen here, the derivatives can play roles as SERMs, tubuline inhibitors, as well as modulators of amino acid metabolism, AhR signaling, and ferroptosis. The relevance of these derivatives as significant antiestrogen molecules demands functional investigations which will clearly provide useful information in the therapy of breast cancer.

Declaration of Competing Interest

The authors declare that they have no known competing financial interests or personal relationships that could have appeared to influence the work reported in this paper.

Acknowledgements

The work was supported by TUBITAK (grant number: 1001 - 213S037).

Appendix A. Supplementary material

Supplementary data to this article can be found online at <https://doi.org/10.1016/j.bioorg.2020.103929>. These data include MOL files and InChIKeys of the most important compounds described in this article.

References

- [1] V.N.R. Gajulapalli, V.L. Malisetty, S.K. Chitta, B. Manavathi, Oestrogen receptor negativity in breast cancer: a cause or consequence? *Biosci. Rep.* 36 (6) (2016).
- [2] I. Paterni, C. Granchi, J.A. Katzenellenbogen, F. Minutolo, Estrogen receptors alpha (ERα) and beta (ERβ): subtype-selective ligands and clinical potential, *Steroids* 90 (2014) 13–29.
- [3] H.-R. Lee, T.-H. Kim, K.-C. Choi, Functions and physiological roles of two types of estrogen receptors, ERα and ERβ, identified by estrogen receptor knockout mouse, *Lab. Anim. Res.* 28 (2) (2012) 71–76.
- [4] M. Madeira, A. Mattar, A.F. Logullo, F.A. Soares, L.H. Gebrim, Estrogen receptor alpha/beta ratio and estrogen receptor beta as predictors of endocrine therapy responsiveness—a randomized neoadjuvant trial comparison between anastrozole and tamoxifen for the treatment of postmenopausal breast cancer, *BMC Cancer* 13 (1) (2013) 425.
- [5] M. Kian Tee, I. Rogatsky, C. Tzagarakis-Foster, A. Cvorov, J. An, R.J. Christy, K.R. Yamamoto, D.C. Leitman, Estradiol and selective estrogen receptor modulators differentially regulate target genes with estrogen receptors α and β, *Mol. Biol. Cell* 15 (3) (2004) 1262–1272.
- [6] J. Russo, I.H. Russo, Toward a physiological approach to breast cancer prevention, *Cancer Epidemiol. Prevent. Biomarkers* 3 (4) (1994) 353–364.
- [7] E.V. Jensen, G. Cheng, C. Palmieri, S. Saji, S. Mäkelä, S. Van Noorden, T. Wahlström, M. Warner, R.C. Coombes, J.-Å. Gustafsson, Estrogen receptors and proliferation markers in primary and recurrent breast cancer, *Proc. Natl. Acad. Sci.* 98 (26) (2001) 15197–15202.
- [8] S. Mann, R. Laucirica, N. Carlson, P.S. Younes, N. Ali, A. Younes, Y. Li, M. Younes, Estrogen receptor beta expression in invasive breast cancer, *Hum. Pathol.* 32 (1) (2001) 113–118.
- [9] E.B.C.T.C. Group, Effects of chemotherapy and hormonal therapy for early breast cancer on recurrence and 15-year survival: an overview of the randomised trials, *Lancet* 365 (9472) (2005) 1687–1717.
- [10] T. Barkhem, B. Carlsson, Y. Nilsson, E. Enmark, J.-Å. Gustafsson, S. Nilsson, Differential response of estrogen receptor α and estrogen receptor β to partial estrogen agonists/antagonists, *Mol. Pharmacol.* 54 (1) (1998) 105–112.
- [11] J. An, C. Tzagarakis-Foster, T.C. Scharschmidt, N. Lomri, D.C. Leitman, Estrogen

- receptor β -selective transcriptional activity and recruitment of coregulators by phytoestrogens, *J. Biol. Chem.* 276 (21) (2001) 17808–17814.
- [12] P.D. Delmas, N.H. Bjarnason, B.H. Mitlak, A.-C. Ravoux, A.S. Shah, W.J. Huster, M. Draper, C. Christiansen, Effects of raloxifene on bone mineral density, serum cholesterol concentrations, and uterine endometrium in postmenopausal women, *N. Engl. J. Med.* 337 (23) (1997) 1641–1647.
- [13] J. Frasar, F. Stossi, J.M. Danes, B. Komm, C.R. Lyttle, B.S. Katzenellenbogen, Selective estrogen receptor modulators: discrimination of agonistic versus antagonistic activities by gene expression profiling in breast cancer cells, *Cancer Res.* 64 (4) (2004) 1522–1533.
- [14] J.S. Lewis-Wambi, H. Kim, R. Curpan, R. Grigg, M.A. Sarker, V.C. Jordan, The selective estrogen receptor modulator bazedoxifene inhibits hormone-independent breast cancer cell growth and down-regulates estrogen receptor α and cyclin D1, *Mol. Pharmacol.* 80 (4) (2011) 610–620.
- [15] S. Martinkovich, D. Shah, S.L. Planey, J.A. Arnott, Selective estrogen receptor modulators: tissue specificity and clinical utility, *Clin. Interv. Aging* 9 (2014) 1437.
- [16] Y.M. Yoo, E.B. Jeung, Melatonin-induced estrogen receptor α -mediated calbindin-D9k expression plays a role in H2O2-mediated cell death in rat pituitary GH3 cells, *J. Pineal Res.* 47 (4) (2009) 301–307.
- [17] F. Payton-Stewart, S.L. Tilghman, L.G. Williams, L.L. Winfield, Benzimidazoles diminish ERE transcriptional activity and cell growth in breast cancer cells, *Biochem. Biophys. Res. Commun.* 450 (4) (2014) 1358–1362.
- [18] N.V. Puranik, P. Srivastava, G. Bhatt, D.J.S.J. Mary, A.M. Limaye, J. Sivaraman, Determination and analysis of agonist and antagonist potential of naturally occurring flavonoids for estrogen receptor (ER α) by various parameters and molecular modelling approach, *Sci. Rep.* 9 (1) (2019) 7450.
- [19] X. Pang, W. Fu, J. Wang, D. Kang, L. Xu, Y. Zhao, A.-L. Liu, G.-H. Du, Identification of estrogen receptor α antagonists from natural products via in vitro and in silico approaches, *Oxid. Med. Cell. Longevity* 2018 (2018).
- [20] K.C. Chang, Y. Wang, P.V. Bodine, S. Nagpal, B.S. Komm, Gene expression profiling studies of three SERMs and their conjugated estrogen combinations in human breast cancer cells: insights into the unique antagonistic effects of bazedoxifene on conjugated estrogens, *J. Steroid Biochem. Mol. Biol.* 118 (1–2) (2010) 117–124.
- [21] E. March-Vila, L. Pinzi, N. Sturm, A. Tinivella, O. Engkvist, H. Chen, G. Rastelli, On the integration of in silico drug design methods for drug repurposing, *Front. Pharmacol.* 8 (2017) 298.
- [22] A.R. El, H.Y. Aboul-Enein, Benzimidazole derivatives as potential anticancer agents, *Mini Rev. Med. Chem.* 13 (3) (2013) 399–407.
- [23] E. Moriarty, M. Carr, S. Bonham, M.P. Carty, F. Aldabbagh, Synthesis and toxicity towards normal and cancer cell lines of benzimidazolequinones containing fused aromatic rings and 2-aromatic ring substituents, *Eur. J. Med. Chem.* 45 (9) (2010) 3762–3769.
- [24] S. Demiryayak, I. Kayagil, L. Yurttas, Microwave supported synthesis of some novel 1, 3-Diarylpiperazine [1, 2-a] benzimidazole derivatives and investigation of their anticancer activities, *Eur. J. Med. Chem.* 46 (1) (2011) 411–416.
- [25] S.M. Sondhi, R. Rani, J. Singh, P. Roy, S. Agrawal, A. Saxena, Solvent free synthesis, anti-inflammatory and anticancer activity evaluation of tricyclic and tetracyclic benzimidazole derivatives, *Bioorg. Med. Chem. Lett.* 20 (7) (2010) 2306–2310.
- [26] I. Kerimov, G. Ayhan-Kilcigil, B. Can-Eke, N. Altanlar, M. İscan, Synthesis, antifungal and antioxidant screening of some novel benzimidazole derivatives, *J. Enzyme Inhib. Med. Chem.* 22 (6) (2007) 696–701.
- [27] M. Rashid, A. Husain, R. Mishra, Synthesis of benzimidazoles bearing oxadiazole nucleus as anticancer agents, *Eur. J. Med. Chem.* 54 (2012) 855–866.
- [28] D. Sharma, B. Narasimhan, P. Kumar, V. Judge, R. Narang, E. De Clercq, J. Balzarini, Synthesis, antimicrobial and antiviral activity of substituted benzimidazoles, *J. Enzyme Inhib. Med. Chem.* 24 (5) (2009) 1161–1168.
- [29] B.V.S. Kumar, S.D. Vaidya, R.V. Kumar, S.B. Bhirud, R.B. Mane, Synthesis and anti-bacterial activity of some novel 2-(6-fluorochroman-2-yl)-1-alkyl/acyl/aryl-1H-benzimidazoles, *Eur. J. Med. Chem.* 41 (5) (2006) 599–604.
- [30] Ö.Ö. Güven, T. Erdoğan, H. Göker, S. Yıldız, Synthesis and antimicrobial activity of some novel phenyl and benzimidazole substituted benzyl ethers, *Bioorg. Med. Chem. Lett.* 17 (8) (2007) 2233–2236.
- [31] E. El-Sawy, F. Bassyouni, S. Abu-Bakr, H. Rady, M. Abdlla, Synthesis and biological activity of some new 1-benzyl and 1-benzoyl-3-heterocyclic indole derivatives, *Acta Pharmaceutica* 60 (1) (2010) 55–71.
- [32] N.I. Ziedan, F. Stefanelli, S. Fogli, A.D. Westwell, Design, synthesis and proapoptotic antitumor properties of indole-based 3, 5-disubstituted oxadiazoles, *Eur. J. Med. Chem.* 45 (10) (2010) 4523–4530.
- [33] N. Misra, R. Luthra, S. Kumar, Enzymology of indole alkaloid biosynthesis in *Catharanthus roseus*, *Indian J. Biochem. Biophys.* 33 (4) (1996) 261–273.
- [34] T. Golob, R. Liebl, E. von Angerer, Sulfamoyloxy-substituted 2-phenylindoles: antiestrogen-based inhibitors of the steroid sulfatase in human breast cancer cells, *Bioorg. Med. Chem.* 10 (12) (2002) 3941–3953.
- [35] R. Mohan, M. Banerjee, A. Ray, T. Manna, L. Wilson, T. Owa, B. Bhattacharyya, D. Panda, Antimitotic sulfonamides inhibit microtubule assembly dynamics and cancer cell proliferation, *Biochemistry* 45 (17) (2006) 5440–5449.
- [36] B.G. Trogden, S.H. Kim, S. Lee, J.A. Katzenellenbogen, Tethered indoles as functionalizable ligands for the estrogen receptor, *Bioorg. Med. Chem. Lett.* 19 (2) (2009) 485–488.
- [37] K. Shah, S. Chhabra, S.K. Shrivastava, P. Mishra, Benzimidazole: a promising pharmacophore, *Med. Chem. Res.* 22 (11) (2013) 5077–5104.
- [38] Y. Bansal, O. Silakari, The therapeutic journey of benzimidazoles: a review, *Bioorg. Med. Chem.* 20 (21) (2012) 6208–6236.
- [39] R. Singla, K.B. Gupta, S. Upadhyay, M. Dhiman, V. Jaitak, Design, synthesis and biological evaluation of novel indole-benzimidazole hybrids targeting estrogen receptor α (ER- α), *Eur. J. Med. Chem.* 146 (2018) 206–219.
- [40] A. Adejare, I. Mercier, Z. Ates-Alagoz, Compounds and compositions for treatment of breast cancer, Google Patents, 2018.
- [41] E.-Y. Moon, S.-K. Seong, S.-H. Jung, M. Lee, D.-K. Lee, D.-K. Rhee, S. Pyo, S.-J. Yoon, Antitumor activity of 4-phenyl-1-arylsulfonylimidazolidinone, DW2143, *Cancer Lett.* 140 (1–2) (1999) 177–187.
- [42] Z. Ates-Alagoz, N. Coleman, M. Martin, A. Wan, A. Adejare, Syntheses and in vitro anticancer properties of novel radiosensitizers, *Chem. Biol. Drug Des.* 80 (6) (2012) 853–861.
- [43] H. Goeker, M. Alp, Z. Ates-Alagoz, S. Yıldız, Synthesis and potent antifungal activity against *Candida* species of some novel 1H-benzimidazoles, *J. Heterocycl. Chem.* 46 (5) (2009) 936–948.
- [44] H. Göker, C. Kuş, D.W. Boykin, S. Yıldız, N. Altanlar, Synthesis of some new 2-substituted-phenyl-1H-benzimidazole-5-carbonitriles and their potent activity against *Candida* species, *Bioorg. Med. Chem.* 10 (8) (2002) 2589–2596.
- [45] Z. Ates-Alagoz, C. Kuş, T. Çoban, Synthesis and antioxidant properties of novel benzimidazoles containing substituted indole or 1, 1, 4, 4-tetramethyl-1, 2, 3, 4-tetrahydro-naphthalene fragments, *J. Enzyme Inhib. Med. Chem.* 20 (4) (2005) 325–331.
- [46] N.A. Clark, M. Hafner, M. Kouril, E.H. Williams, J.L. Muhlich, M. Pilarczyk, M. Niepel, P.K. Sorger, M. Medvedovic, GRcalculator: an online tool for calculating and mining dose–response data, *BMC Cancer* 17 (1) (2017) 698.
- [47] D.S. Goodsell, C. Zardecki, L. Di Costanzo, J.M. Duarte, B.P. Hudson, I. Persikova, J. Segura, C. Shao, M. Voigt, J.D. Westbrook, RCSB Protein Data Bank: Enabling biomedical research and drug discovery, *Protein Sci.* 29 (1) (2020) 52–65.
- [48] S. Epik, LLC, New York, NY, 2016; Impact, Schrödinger, LLC, New York, NY, 2016; Prime, Schrödinger, LLC, New York, NY, 2019, Schrödinger Release 2019-3: Protein Preparation Wizard, LLC, New York.
- [49] L. Schrödinger, New York, NY, 2019, Schrödinger Release 2019-3: Maestro.
- [50] L. Schrödinger, New York, NY, 2019, Schrödinger Release 2019-3: LigPrep.
- [51] D.S. Wishart, Y.D. Feunang, A.C. Guo, E.J. Lo, A. Marcu, J.R. Grant, T. Sajed, D. Johnson, C. Li, Z. Sayeeda, DrugBank 5.0: a major update to the DrugBank database for 2018, *Nucleic Acids Res.* 46(D1) (2018) D1074–D1082.
- [52] L. Schrödinger, New York, NY, 2019, Schrödinger Release 2019-3: Glide.
- [53] L. Schrödinger, New York, NY, 2019, Schrödinger Release 2019-3: QikProp.
- [54] L. Gautier, L. Cope, B.M. Bolstad, R.A. Irizarry, affy—analysis of Affymetrix GeneChip data at the probe level, *Bioinformatics* 20 (3) (2004) 307–315.
- [55] M.E. Ritchie, B. Phipson, D. Wu, Y. Hu, C.W. Law, W. Shi, G.K. Smyth, limma powers differential expression analyses for RNA-sequencing and microarray studies, *Nucleic Acids Res.* 43 (7) (2015) e47.
- [56] M. Kanehisa, M. Furumichi, M. Tanabe, Y. Sato, K. Morishima, KEGG: new perspectives on genomes, pathways, diseases and drugs, *Nucleic Acids Res.* 45 (D1) (2016) D353–D361.
- [57] V. Stathias, A. Koletti, D. Vidović, D.J. Cooper, K.M. Jagodnik, R. Terryn, M. Forlin, C. Chung, D. Torre, N. Ayad, Sustainable data and metadata management at the BD2K-LINCS Data Coordination and Integration Center, *Sci. Data* 5 (2018) 180117.
- [58] D. Szklarczyk, A. Franceschini, S. Wyder, K. Forslund, D. Heller, J. Huerta-Cepas, M. Simonovic, A. Roth, A. Santos, K.P. Tsafou, STRING v10: protein–protein interaction networks, integrated over the tree of life, *Nucleic Acids Res.* 43 (D1) (2014) D447–D452.
- [59] V.U.-B.E. Genomics, Calculate and draw custom Venn diagrams. <http://bioinformatics.psb.ugent.be/webtools/Venn/>. (Accessed March 10 2020).
- [60] W.K. Lim, K. Wang, C. Lefebvre, A. Califano, Comparative analysis of microarray normalization procedures: effects on reverse engineering gene networks, *Bioinformatics* 23 (13) (2007) i282–i288.
- [61] Q. Li, N.J. Birkbak, B. Györfy, Z. Szallasi, A.C. Eklund, Jetset: selecting the optimal microarray probe set to represent a gene, *BMC Bioinf.* 12 (1) (2011) 474.
- [62] Z. Gu, R. Eils, M. Schlesner, Complex heatmaps reveal patterns and correlations in multidimensional genomic data, *Bioinformatics* 32 (18) (2016) 2847–2849.
- [63] Z. Ates-Alagoz, Z. Buyukbingol, E. Buyukbingol, Synthesis and antioxidant properties of some indole ethylamine derivatives as melatonin analogs, *Die Pharmazie-Int. J. Pharm. Sci.* 60 (9) (2005) 643–647.
- [64] A.K. Shiau, D. Barstad, P.M. Loria, L. Cheng, P.J. Kushner, D.A. Agard, G.L. Greene, The structural basis of estrogen receptor/coactivator recognition and the antagonism of this interaction by tamoxifen, *Cell* 95 (7) (1998) 927–937.
- [65] M. Niklasson, G. Maddalo, Z. Sramkova, E. Mutlu, S. Wee, P. Sekyrova, L. Schmidt, N. Frits, I. Dehnisch, G. Kyriatzi, Membrane-polarizing channel blockers induce selective glioma cell death by impairing nutrient transport and unfolded protein/amino acid responses, *Cancer Res.* 77 (7) (2017) 1741–1752.
- [66] P. Gong, Z. Madak-Erdogan, J.A. Flaws, D.J. Shapiro, J.A. Katzenellenbogen, B.S. Katzenellenbogen, Estrogen receptor- α and aryl hydrocarbon receptor involvement in the actions of botanical estrogens in target cells, *Mol. Cell. Endocrinol.* 437 (2016) 190–200.
- [67] E.L. Hsu, D. Yoon, H.H. Choi, F. Wang, R.T. Taylor, N. Chen, R. Zhang, O. Hankinson, A proposed mechanism for the protective effect of dioxin against breast cancer, *Toxicol. Sci.* 98 (2) (2007) 436–444.
- [68] X. Tang, M.M. Keenan, J. Wu, C.-A. Lin, L. Dubois, J.W. Thompson, S.J. Freedland, S.K. Murphy, J.-T. Chi, Comprehensive profiling of amino acid response uncovers unique methionine-deprived response dependent on intact creatine biosynthesis, *PLoS Genet.* 11 (4) (2015).
- [69] A. Subramanian, P. Tamayo, V.K. Mootha, S. Mukherjee, B.L. Ebert, M.A. Gillette, A. Paulovich, S.L. Pomeroy, T.R. Golub, E.S. Lander, Gene set enrichment analysis: a knowledge-based approach for interpreting genome-wide expression profiles,

- Proc. Natl. Acad. Sci. 102 (43) (2005) 15545–15550.
- [70] M. Kanehisa, Enzyme annotation and metabolic reconstruction using KEGG, Protein Function Prediction, Springer, 2017, pp. 135–145.
- [71] V.K. Mootha, C.M. Lindgren, K.-F. Eriksson, A. Subramanian, S. Sihag, J. Lehara, P. Puigserver, E. Carlsson, M. Ridderstråle, E. Laurila, PGC-1 α -responsive genes involved in oxidative phosphorylation are coordinately downregulated in human diabetes, *Nat. Genet.* 34 (3) (2003) 267.
- [72] G.P. Skloris, E. Leygue, P.H. Watson, L.C. Murphy, Estrogen receptor alpha negative breast cancer patients: estrogen receptor beta as a therapeutic target, *J. Steroid Biochem. Mol. Biol.* 109 (1–2) (2008) 1–10.
- [73] H. Hua, H. Zhang, Q. Kong, Y. Jiang, Mechanisms for estrogen receptor expression in human cancer, *Exp. Hematol. Oncol.* 7 (1) (2018) 1–11.
- [74] M. De Santi, L. Galluzzi, S. Lucarini, M.F. Paoletti, A. Fraternali, A. Duranti, C. De Marco, M. Fanelli, N. Zaffaroni, G. Brandi, The indole-3-carbinol cyclic tetrameric derivative CTet inhibits cell proliferation via overexpression of p21/CDKN1A in both estrogen receptor-positive and triple-negative breast cancer cell lines, *Breast Cancer Res.* 13 (2) (2011) R33.
- [75] L. Galluzzi, M. De Santi, R. Crinelli, C. De Marco, N. Zaffaroni, A. Duranti, G. Brandi, M. Magnani, Induction of endoplasmic reticulum stress response by the indole-3-carbinol cyclic tetrameric derivative CTet in human breast cancer cell lines, *PLoS ONE* 7 (8) (2012) e43249.
- [76] S. Honda, P. Lohar, M. Shigematsu, J.P. Palazzo, R. Suzuki, I. Imoto, I. Rigoutsos, Y. Kirino, Sex hormone-dependent tRNA halves enhance cell proliferation in breast and prostate cancers, *Proc. Natl. Acad. Sci.* 112 (29) (2015) E3816–E3825.
- [77] J. Finlay-Schultz, A.E. Gillen, H.M. Brechbuhl, J.J. Ivie, S.B. Matthews, B.M. Jacobsen, D.L. Bentley, P. Kabos, C.A. Sartorius, Breast cancer suppression by progesterone receptors is mediated by their modulation of estrogen receptors and RNA polymerase III, *Cancer Res.* 77 (18) (2017) 4934–4946.
- [78] I. Katsyv, M. Wang, W.M. Song, X. Zhou, Y. Zhao, S. Park, J. Zhu, B. Zhang, H.Y. Irie, EPRS is a critical regulator of cell proliferation and estrogen signaling in ER+ breast cancer, *Oncotarget* 7 (43) (2016) 69592.
- [79] H. Putzer, S. Laalami, Regulation of the expression of aminoacyl-tRNA synthetases and translation factors, *Madame Curie Bioscience Database [Internet]*, Landes Bioscience, 2013.
- [80] K.A. Dittmar, M.A. Sørensen, J. Elf, M. Ehrenberg, T. Pan, Selective charging of tRNA isoacceptors induced by amino-acid starvation, *EMBO Rep.* 6 (2) (2005) 151–157.
- [81] M. Hayano, W. Yang, C. Corn, N. Pagano, B. Stockwell, Loss of cysteinyl-tRNA synthetase (CARS) induces the transsulfuration pathway and inhibits ferroptosis induced by cystine deprivation, *Cell Death Differ.* 23 (2) (2016) 270–278.
- [82] X. Yu, Y.C. Long, Crosstalk between cystine and glutathione is critical for the regulation of amino acid signaling pathways and ferroptosis, *Sci. Rep.* 6 (1) (2016) 1–11.
- [83] M. Gao, P. Monian, N. Quadri, R. Ramasamy, X. Jiang, Glutaminolysis and transferrin regulate ferroptosis, *Mol. Cell* 59 (2) (2015) 298–308.
- [84] K.K. Brown, J.B. Spinelli, J.M. Asara, A. Toker, Adaptive reprogramming of de novo pyrimidine synthesis is a metabolic vulnerability in triple-negative breast cancer, *Cancer Discov.* 7 (4) (2017) 391–399.
- [85] E. Villa, E.S. Ali, U. Sahu, I. Ben-Sahra, Cancer cells tune the signaling pathways to empower de novo synthesis of nucleotides, *Cancers* 11 (5) (2019) 688.
- [86] E. Kulkoyluoglu-Cotul, A. Arca, Z. Madak-Erdogan, Crosstalk between estrogen signaling and breast cancer metabolism, *Trends Endocrinol. Metab.* 30 (1) (2019) 25–38.
- [87] G.S. Papaetis, K.N. Syrigos, Sunitinib, *BioDrugs* 23 (6) (2009) 377–389.
- [88] Y. Hirata, C. Yamada, Y. Ito, S. Yamamoto, H. Nagase, K. Oh-hashii, K. Kiuchi, H. Suzuki, M. Sawada, K. Furuta, Novel oxindole derivatives prevent oxidative stress-induced cell death in mouse hippocampal HT22 cells, *Neuropharmacology* 135 (2018) 242–252.
- [89] Y. Hirata, T. Iwasaki, Y. Makimura, S. Okajima, K. Oh-hashii, H. Takemori, Inhibition of double-stranded RNA-dependent protein kinase prevents oxytosis and ferroptosis in mouse hippocampal HT22 cells, *Toxicology* 418 (2019) 1–10.
- [90] M. Santoni, C. Amantini, M.B. Morelli, V. Farfariello, M. Nabissi, S. Liberati, L. Bonfili, M. Mozzicafreddo, A.M. Eleuteri, L. Burattini, Different effects of sunitinib, sorafenib, and pazopanib on inducing cancer cell death: The role of autophagy, *Am. Soc. Clin. Oncol.* (2013).
- [91] S.J. Dixon, D.N. Patel, M. Welsch, R. Skouta, E.D. Lee, M. Hayano, A.G. Thomas, C.E. Gleason, N.P. Tatonetti, B.S. Slusher, Pharmacological inhibition of cystine–glutamate exchange induces endoplasmic reticulum stress and ferroptosis, *Elife* 3 (2014) e02523.
- [92] T.D. Hubbard, I.A. Murray, W.H. Bisson, T.S. Lahoti, K. Gowda, S.G. Amin, A.D. Patterson, G.H. Perdew, Adaptation of the human aryl hydrocarbon receptor to sense microbiota-derived indoles, *Sci. Rep.* 5 (1) (2015) 1–13.
- [93] E. Zgheib, A. Limonciel, X. Jiang, A. Wilmes, S. Wink, B. Van De Water, A. Kopp-Schneider, F.Y. Bois, P. Jennings, Investigation of Nrf2, AhR and ATF4 activation in toxicogenomic databases, *Front. Genet.* 9 (2018) 429.
- [94] Y. Cheng, U.-H. Jin, C.D. Allred, A. Jayaraman, R.S. Chapkin, S. Safe, Aryl hydrocarbon receptor activity of tryptophan metabolites in young adult mouse colonocytes, *Drug Metab. Dispos.* 43 (10) (2015) 1536–1543.
- [95] J.K. Tomblin, S. Arthur, D.A. Primerano, A.R. Chaudhry, J. Fan, J. Denvir, T.B. Salisbury, Aryl hydrocarbon receptor (AHR) regulation of L-Type Amino Acid Transporter 1 (LAT-1) expression in MCF-7 and MDA-MB-231 breast cancer cells, *Biochem. Pharmacol.* 106 (2016) 94–103.
- [96] P. Tarnow, T. Tralau, A. Luch, Chemical activation of estrogen and aryl hydrocarbon receptor signaling pathways and their interaction in toxicology and metabolism, *Expert Opin. Drug Metab. Toxicol.* 15 (3) (2019) 219–229.
- [97] P. Maher, K. van Leyen, P.N. Dey, B. Honrath, A. Dolga, A. Methner, The role of Ca²⁺ in cell death caused by oxidative glutamate toxicity and ferroptosis, *Cell Calcium* 70 (2018) 47–55.
- [98] J. Lewerenz, G. Ates, A. Methner, M. Conrad, P. Maher, Oxytosis/ferroptosis—(Re-) emerging roles for oxidative stress-dependent non-apoptotic cell death in diseases of the central nervous system, *Front. Neurosci.* 12 (2018) 214.
- [99] B. Hong, Z. Su, C. Zhang, Y. Yang, Y. Guo, W. Li, A.-N.T. Kong, Reserpine inhibit the JB6 P+ cell transformation through epigenetic reactivation of Nrf2-mediated anti-oxidative stress pathway, *AAPS J.* 18 (3) (2016) 659–669.
- [100] A. Brancale, R. Silvestri, Indole, a core nucleus for potent inhibitors of tubulin polymerization, *Med. Res. Rev.* 27 (2) (2007) 209–238.
- [101] F.C. Torres, M. Eugenia Garcia-Rubino, C. Lozano-Lopez, D.F. Kawano, V.L. Eifler-Lima, G.L. von Poser, J.M. Campos, Imidazoles and benzimidazoles as tubulin-modulators for anti-cancer therapy, *Curr. Med. Chem.* 22 (11) (2015) 1312–1323.
- [102] Y.-T. Wang, Y.-J. Qin, N. Yang, Y.-L. Zhang, C.-H. Liu, H.-L. Zhu, Synthesis, biological evaluation, and molecular docking studies of novel 1-benzene acyl-2-(1-methylindol-3-yl)-benzimidazole derivatives as potential tubulin polymerization inhibitors, *Eur. J. Med. Chem.* 99 (2015) 125–137.
- [103] M. Fantacuzzi, B. De Filippis, M. Gallorini, A. Ammazalorso, L. Giampietro, C. Maccallini, Z. Aturki, E. Donati, R.S. Ibrahim, E. Shawky, Synthesis, biological evaluation, and docking study of indole aryl sulfonamides as aromatase inhibitors, *Eur. J. Med. Chem.* 185 (2020) 111815.